NASA TECHNICAL NOTE

NASA TN D-3673

NASA TN D-3673

WIND-TUNNEL INVESTIGATION OF THE FLIGHT CHARACTERISTICS OF A MODEL OF AN ASPECT-RATIO-6 CONICAL-PARAWING UTILITY VEHICLE

by Charles C. Smith, Jr., and George M. Ware

Langley Research Center
Langley Station, Hampton, Va.

NATIONAL AERONAUTICS AND SPACE ADMINISTRATION • WASHINGTON, D. C. • FEBRUARY 1967

NASA TN D-3673

WIND-TUNNEL INVESTIGATION OF THE FLIGHT CHARACTERISTICS OF A MODEL OF AN ASPECT-RATIO-6 CONICAL-PARAWING UTILITY VEHICLE

By Charles C. Smith, Jr., and George M. Ware

Langley Research Center
Langley Station, Hampton, Va.

Technical Film Supplement L-920 available on request.

NATIONAL AERONAUTICS AND SPACE ADMINISTRATION

For sale by the Clearinghouse for Federal Scientific and Technical Information
Springfield, Virginia 22151 – Price $2.00

WIND-TUNNEL INVESTIGATION OF THE FLIGHT CHARACTERISTICS OF A MODEL OF AN ASPECT-RATIO-6 CONICAL-PARAWING UTILITY VEHICLE

By Charles C. Smith, Jr., and George M. Ware
Langley Research Center

SUMMARY

A low-speed wind-tunnel investigation has been made to determine the flight characteristics of a flying model of a parawing vehicle with a wing having an aspect ratio of 6. Flight tests were made over an angle-of-attack range of the parawing keel from about 23° to 40°. The model consisted basically of a cargo platform attached to a parawing by means of an overhead truss arrangement, and it was powered by a pusher propeller located at the rear of the platform. Control was provided by pitching and rolling the wing and by a rudder surface mounted in the propeller slipstream.

The results of the investigation showed that the model had satisfactory dynamic longitudinal and lateral stability, and the motions were well damped over the angle-of-attack range of the tests. The center-of-gravity-shift control system was reasonably effective for controlling the model but was considered relatively weak and was generally rated low in terms of conventional airplane control power requirements. Because of the good stability, however, this relatively weak control was generally satisfactory for maintaining wing-level flight and for performing the mild maneuvers possible in the tunnel.

INTRODUCTION

The National Aeronautics and Space Administration has conducted a number of investigations to determine the aerodynamic characteristics of parawing configurations. (For example, see refs. 1 to 5.) The parawing which received the most attention in these studies was of low aspect ratio and had a conical canopy with equal-length leading edges and keel. The low-aspect-ratio conical parawing may be adequate for applications in which only a moderate glide range is required. For other applications, such as tow vehicles or utility-type vehicles, or where extended glide range is needed, however, a wing with a higher lift-drag ratio would be desirable.

Previous work on parawings has shown that increases in aspect ratio from 3 to about 6 gave appreciable increases in maximum lift-drag ratio particularly for parawings with cylindrical canopies. For parawings with conical canopies, the increase in maximum

lift-drag ratio with increasing aspect ratio was not as pronounced but appreciable improvements in longitudinal and directional stability and control characteristics could be achieved. (See refs. 1 and 2.)

The present investigation was conducted to study the low-speed dynamic stability and control characteristics of an aspect-ratio-6 conical parawing. These tests consisted of low-speed force and flight tests conducted in the test section of the Langley full-scale tunnel. The aspect-ratio-6 configuration differs from the more conventional (low-aspect-ratio) parawing in that the length of the keel was considerably less than the lengths of the leading edges. The model was generally similar in design to the parawing vehicles tested in previous investigations (refs. 4 and 5) in that it consisted basically of a cargo platform (the same platform as that used in ref. 4) attached to a parawing by means of an overhead truss arrangement. It was powered by a pusher propeller located at the rear of the platform. The vehicle was controlled by banking the wing for roll control, pitching the wing for pitch control, and deflecting a rudder mounted in the slipstream of the propeller for yaw control.

In the present investigation, flight tests were made to determine the dynamic stability and control characteristics of the model over an angle-of-attack range of the parawing keel from about 23° up to the maximum trim angle of attack possible (40°) with the design control system. Static force tests were made over a keel angle-of-attack range of 15° to 50° to determine the static stability and control characteristics of the model for correlation with the flight-test results.

Motion-picture film supplement L-920 has been prepared and is available on loan. A request card and a description of the film are included at the back of this document.

SYMBOLS

All forces, moments, and velocities with the exception of lift and drag are presented with respect to a system of body axes. For the complete model, the body-axis system was parallel to the cargo bed and originated at the reference center of gravity. (See fig. 1.) For wing-alone tests, the body-axis system was parallel to the parawing keel and originated at the wing pivot point. All measurements are reduced to standard coefficient form and are based on the flat pattern (45° leading-edge sweep) dimensional characteristics of the wing. Equivalent values in the International System (SI) are also indicated herein. See reference 6 for (SI) physical constants and conversion factors.

b wing span, ft (m)

C_D drag coefficient, F_D/qS

C_L lift coefficient, F_L/qS

C_l rolling-moment coefficient, M_X/qSb

$\Delta C_l, \Delta C_n, \Delta C_Y$ incremental force and moments

$C_{l_\beta} = \frac{\partial C_l}{\partial \beta}$, per degree

C_m pitching-moment coefficient, M_Y/qSl_k

$C_{m,o}$ pitching-moment coefficient at zero lift, $M_{Y,o}/qSl_k$

C_n yawing-moment coefficient, M_Z/qSb

$C_{n_\beta} = \frac{\partial C_n}{\partial \beta}$, per degree

C_T thrust coefficient, $\left[C_{D_{(\text{power-on})}} - C_{D_{(\text{power-off, propeller windmilling})}}\right]_{\alpha_p=0}$

C_Y lateral-force coefficient, F_Y/qS

$C_{Y_\beta} = \frac{\partial C_Y}{\partial \beta}$, per degree

F_D drag, lbf (N)

F_L lift, lbf (N)

F_Y side force, lbf (N)

I_X moment of inertia about X-axis, slug-ft^2 (kg-m^2)

I_Y moment of inertia about Y-axis, slug-ft^2 (kg-m^2)

I_Z moment of inertia about Z-axis, slug-ft^2 (kg-m^2)

i_w	angle of incidence of parawing keel angle with respect to platform, $\alpha_k - \alpha_p$, deg
L/D	lift-drag ratio
ℓ_k	keel length, ft (m)
M_X	rolling moment, ft-lb (m-N)
M_Y	pitching moment, ft-lb (m-N)
$M_{Y,o}$	pitching moment at zero lift, ft-lb (m-N)
M_Z	rolling moment, ft-lb (m-N)
q	free-stream dynamic pressure, lb/sq ft (N/m^2)
S	wing area, sq ft (m^2)
X, Y, Z	longitudinal, lateral, and normal body axes, respectively
z	distance along Z-body axes, ft (m)
α_k	angle of attack of keel, deg
α_p	angle of attack of platform, deg
β	angle of sideslip, $-\psi$, deg
δ_r	deflection of rudder surface, positive trailing edge left, deg
ϕ	angle of roll, positive right wing tip down, deg
ψ	angle of yaw, deg

Subscript:

max	maximum

MODEL AND APPARATUS

A photograph of the model flying in the tunnel is presented in figure 2 and sketches showing some of the more important model dimensions are presented in figure 3. Additional dimensional and mass characteristics of the model are presented in the following table:

Weight	72 lb	(320.27 N)
Wing loading	2.87 lb/sq ft	(137.42 N/m^2)
Moment of inertia:		
I_X	7.67 slug-ft^2	(10.40 kg-m^2)
I_Y	9.72 slug-ft^2	(13.18 kg-m^2)
I_Z	7.67 slug-ft^2	(10.40 kg-m^2)
Parawing dimensions:		
Area (flat pattern, 45° leading-edge sweep)	25.225 sq ft	(2.34 m^2)
Span (flat pattern, 45° leading-edge-sweep condition)	12.08 ft	(3.68 m)
Keel length	4.10 ft	(1.25 m)
Rudder dimensions:		
Area	1.50 sq ft	(0.14 m^2)
Span	2.00 ft	(0.61 m)
Chord	0.75 ft	(0.23 m)

The test vehicle was similar to the earlier vehicles used in previous parawing investigations (refs. 4 and 5) in that it consisted basically of a cargo platform attached to a parawing by means of an overhead truss arrangement. It was powered by a pusher propeller located at the rear of the platform and had a cockpit located at the front. A parawing having an aspect ratio of 6 and a conical canopy was used on the vehicle. The keel of the wing was constructed of an aluminum-alloy box beam and the two airfoil-shaped leading edges were constructed of aluminum tubing covered with balsa wood. The leading edges were hinged together at the apex of the wing. The aspect-ratio-6 parawing differs from the more conventional (low-aspect-ratio) parawing in that the length of the keel was considerably less than the lengths of the leading edges. A fixed leading-edge sweep angle of 50° was maintained by a spreader bar which was attached to the parawing leading edges and to the keel at approximately the 72-percent keel station.

When the leading edges were spread out until the fabric assumed a flat pattern, the trailing edges of the fabric were straight from the wing tips to the keel and the leading-edge sweep angle was 45°. The fabric used to form the membrane of the parawing was made of nylon cloth with a plastic coating to give essentially zero porosity. The wing pivot was located so that the resultant force of the wing-alone lift and drag would act approximately through the center of gravity of the complete model.

Pitch and roll control for the model were obtained by pitching and banking the wing, respectively (which is, in effect, control by a center-of-gravity shift). Yaw control was provided by a rudder surface mounted directly in the propeller slipstream.

Electrically operated servoactuators mounted on the platform were used to provide control deflections in response to electrical signals generated by the pilot's control stick. The control used was of the full-off and full-on type in that deflection of the control stick caused surfaces to be deflected to a predetermined deflection at a fixed rate (depending upon the gearing and linkage involved). When the control stick was released, the control surfaces returned to their neutral setting.

Thrust for the model was supplied by a pneumatic motor driving a four-blade pusher propeller. The propeller blades had 3-inch chords and were set at a blade angle of 14° measured at the 0.75-radius station.

The investigation was conducted in the Langley full-scale tunnel. The flight tests were made by using the technique described in reference 7 and the equipment illustrated in figure 4. Static force tests were made by using a single-strut support and a strain-gage balance.

TESTS

Flight Tests

Flight tests were made to study the dynamic stability and control characteristics of the model over a range of keel angle of attack from 23° to 40°, which corresponded to an airspeed range from about 24 to 38 knots. The wing bank angle used for roll control was $\pm 5^{\circ}$. The rudder surface was deflected $\pm 20^{\circ}$ for yaw control. At each trim airspeed the model was flown by using rudder alone, wing bank alone, and coordinated rudder and wing bank for lateral control.

The longitudinal location of the center of gravity for the flight tests was 2.60 inches (6.60 cm) forward of and 0.8 inch (2.03 cm) above the reference center-of-gravity location shown in figure 3, which was the moment reference center for the force tests.

The stability, controllability, and the general flight behavior of the model were determined in various cases, either qualitatively from the pilots' observations or quantitatively from motion-picture records of the flights. General flight behavior is the term used to describe the overall flying characteristics of a model and indicates the ease with which the model can be flown. In effect, the general flight behavior is much the same as that indicated by the pilot's opinion of the flying qualities of an airplane and indicates whether stability and controllability are adequate and properly proportioned.

Force Tests

For all the force tests, the strain-gage balance was mounted so that its longitudinal axis was alined with the cargo platform. The balance moment center was located at the reference center of gravity shown in figure 3. Since the forces and moments were therefore measured with respect to the platform angle, it was more convenient to use this angle rather than the keel angle as reference for angle of attack. For this reason, the data are plotted in terms of platform angle and are discussed in terms of this angle except for a few cases where the data are referred to the keel angle for comparison purposes. For the wing-alone (including the spreader bar) force tests, the balance was mounted so that its longitudinal axis was alined with the keel and the moments were referred to the wing pivot point.

Power-off and power-on force tests were made to determine the static longitudinal and lateral stability and control characteristics of the model for use in correlation with the flight-test results. In the power-off tests, the propeller was allowed to windmill. In the power-on longitudinal tests, an effort was made in some cases to simulate steady level flight by trimming the model in both pitch and drag.

Most of the force tests were made over an angle-of-attack range of the platform from -10° to 20° for wing incidences of 20°, 25°, and 30°. (The angle-of-attack range of the keel covered by this group of tests varied from 15° to 50°.) The lateral tests were made for sideslip angles of $\pm 5^{\circ}$. The tests to determine the lateral control effectiveness of the wing were made for wing bank angles of $\pm 5^{\circ}$ to $\pm 10^{\circ}$ relative to the body axis of the platform. Tests made to determine the effectiveness of the rudder surface were made for deflections of $\pm 10^{\circ}$ to $\pm 20^{\circ}$. In addition to these tests of the complete model, a few tests were also made with the wing alone.

All the tests were made at a dynamic pressure of about 2.87 pounds per square foot (137.42 N/m^2) which corresponds to an airspeed of 28.1 knots to a Reynolds number of 891 529 based on the parawing keel length of 2.96 feet (0.902 m).

RESULTS AND DISCUSSION

Force Tests

Static longitudinal stability and trim.- The results of force tests to determine the static longitudinal stability and trim characteristics of the model are presented in figure 5 for wing incidences of 20°, 25°, and 30°. These data show that the model has static longitudinal stability throughout the angle-of-attack range and that for the 25° and 30° wing incidence cases, the stability increased somewhat after the stall. The data also show that power increased the maximum lift coefficient and that there was little or no change in the longitudinal stability due to power.

In order to permit a comparison of the effects of wing incidence on the longitudinal characteristics to be made more conveniently, the data of figure 5 for i_w conditions of 20^o, 25^o, and 30^o are replotted in figure 6 for the power-off case. Figure 6(a) shows the data plotted against the angle of attack of the platform, and figure 6(b) shows the data plotted against angle of attack of the keel. Also presented in figure 6(a) are data for the model with the parawing off obtained from reference 4 and corrected for the difference in wing area and keel length. The data of figure 6(b) show that the lift and drag characteristics of the vehicle at the three angles of incidence are almost identical when compared on the basis of equal wing angle of attack. This result indicates that the angle of attack of the platform had little effect on the lift or drag. The angle of the platform relative to the wing did, however, have a pronounced effect on the pitching moments since changing the incidence moved the center of gravity relative to the wing. For example, increasing the wing incidence moved the center of gravity rearward relative to the wing and both reduced the static longitudinal stability and increased the trim angle of attack.

The maximum trimmed value of L/D for the complete model obtained for the $i_w = 20^o$ condition at a lift coefficient of about 0.90 was about 3.1. This value of maximum trimmed L/D is considerably less than the value of 4.2 achieved with the same basic model with a lower aspect ratio wing in reference 4. There are two factors which, taken together, explain this apparent discrepancy of a lower L/D with the higher aspect ratio wing: (1) the higher aspect ratio wing had about the same value of L/D for the wing alone as did the lower aspect ratio wing, and (2) the higher aspect ratio wing was smaller, having the same span and less chord; thus its lifting capability was reduced whereas the drag of the platform remained the same. The fact that the higher aspect ratio wing did not have any significantly higher L/D than did the lower aspect ratio wing is illustrated in figure 7 by the results for wing-alone tests of the two wings. These data at two different values of dynamic pressure show no consistent difference in the value of $(L/D)_{max}$ for the two wings. This result is generally in good agreement with the data presented in reference 2 where it was shown that on conical wings, increasing the aspect ratio from about 3 to 5.5 produced only a very small gain in $(L/D)_{max}$.

The data of figure 7 show that the wing-alone pitching moments about the wing pivot generally indicate stability for both wings and that the aspect-ratio-6 wings have positive values of $C_{m,o}$ whereas the aspect-ratio-3 wing has negative values of $C_{m,o}$. This result is in agreement with the data of references 1, 2, and 3 and is of significance because in the center-of-gravity-shift control system, the sign of $C_{m,o}$ determines the sign of the stick-force gradient. A positive value of $C_{m,o}$ provides a stable stick-force variation with speed (that is, pull force is required for trim at the lower speeds and a push force at the higher speeds) whereas an unstable variation is obtained when $C_{m,o}$ is negative. (See ref. 5.) From longitudinal control considerations, therefore, the

high-aspect-ratio wing is more desirable than the low-aspect-ratio wing when the center-of-gravity-shift control system is employed.

Static lateral stability and control.- The results of force tests to determine the static lateral stability characteristics of the model are presented in figure 8 for wing incidences of 20°, 25°, and 30°, and sideslip angles of $\pm 5^{\circ}$ and are compared with corresponding data taken from reference 4 for an aspect-ratio-3 wing with a conical canopy. These data for the model with the aspect-ratio-6 wing are summarized in figure 9 in terms of keel angle of attack for the power-off condition. The data of figure 8 show that the model has static directional stability C_{n_β} and positive effective dihedral $-C_{l_\beta}$ throughout the angle-of-attack range except for the $i_w = 30^{\circ}$ power-off case where the model becomes directionally unstable at the high angles of attack – angles well above the stall. These data also show that, in general, power improved the directional stability of the model. The greatest effect of power occurred at the high angle of attack for the $i_w = 30^{\circ}$ case where the directional stability changed from unstable $-C_{n_\beta}$ to stable C_{n_β}.

Comparison of the data for the model with aspect-ratio-3 and aspect-ratio-6 wings (fig. 8) shows that, in general, the model with the aspect-ratio-6 wing had more directional stability C_{n_β} and less positive effective dihedral $-C_{l_\beta}$ than the model with the aspect-ratio-3 wing.

The data of figure 9 show that there is little effect of i_w on the lateral stability characteristics of the model and that, in general, increasing the angle of attack of the keel α_k increased C_{n_β} for values of α_k up to a value of 20° to 25°. Further increases in α_k resulted in a gradual reduction of C_{n_β} until at the high angles of attack, the model became directionally unstable.

The results of force tests made to determine the static lateral stability characteristics of the parawing alone are presented in figure 10. Data for the aspect-ratio-3 wing of reference 4 are also plotted in figure 10 for comparison purposes. These data are referred to a reference point at the keel axis and to a system of axes parallel to the keel axis and therefore are not directly comparable to the data for the complete model. These data show that the directional stability of the aspect-ratio-6 wing was much higher than that of the aspect-ratio-3 wing as would be expected on the basis of previous work. The dihedral effect for the two wings was of about the same level and showed a similar variation with angle of attack.

The static incremental lateral control characteristics produced by banking the parawing with respect to the platform are presented in figure 11 for $\phi = 5^{\circ}$ and in figure 12 for $\phi = 10^{\circ}$ for i_w conditions of 20°, 25°, and 30°. These data are summarized in figure 13 for the power-off case since power had little or no effect on the basic data. The data of figure 13(a) show that banking the wing $\pm 5^{\circ}$ produced favorable rolling moments and

yawing moments that were slightly adverse at low and high angles of attack and slightly favorable at moderate angles of attack. The data of figure 13(b) show that increasing the wing bank angles to 10° gave higher favorable rolling moments but also gave higher adverse yawing moments.

The investigation of reference 4 pointed out that in wind-tunnel tests in which the platform of the model remained fixed and the wing was banked, there was considerable difference in static control characteristics depending upon the axis about which the wing was banked (keel axis or platform axis). If the static roll-control data for these two cases are compared, it will be found that wing bank about an axis parallel to the keel produces relatively small rolling moments but favorable yawing moments whereas wing bank about an axis parallel to the platform, as was the case in the present investigation, produces relatively high rolling moments but adverse yawing moments. Under actual flight conditions the overall control effectiveness is believed to be about the same for the two cases inasmuch as yawing moments produce sideslip and this sideslip acting through the effective dihedral parameter C_{l_β} produces rolling moments that tend to equalize the net rolling moment acting in the two cases.

In reference 8 an expression for easily calculating the net rolling-moment coefficient $C_{l,\text{net}}$ (rolling moment for the case of zero yawing moment) for configurations employing a wing-bank control system was derived. This expression

$$\Delta C_{l,\text{net}} = \frac{z}{b} C_L \sin\phi\left(1 + \frac{C_{l_\beta}}{C_{n_\beta}} \frac{1}{L/D}\right)$$

was used to calculate the net rolling-moment coefficient produced by 5° wing bank for the model of the present investigation and the results are presented in figure 14. Also shown in figure 14 is a plot of the net rolling-moment coefficient for the aspect-ratio-3 wing. The data show that the net rolling moments are very nearly equal to the measured rolling moments for the aspect-ratio-6 wing and remain fairly constant with angle of attack whereas the net rolling moments for the aspect-ratio-3 wing are considerably below the measured rolling moments and show a rapid dropoff at the higher angles of attack. This much larger difference between the measured and net rolling moments for the aspect-ratio-3 wing is the result of its much lower directional stability and much more adverse yawing moments.

Presented in figure 15 are the results of tests to determine the lateral control effectiveness of the vertical rudder surface mounted directly in the slipstream. These data show that incremental yawing moments produced by the rudder were small in the power-off case, but, as would be expected, were relatively large for the power-on condition.

Flight Tests

Longitudinal stability and control.- The model was found to have dynamic longitudinal stability and the motions were well damped over the angle-of-attack range (23° to 40°). The decrease in the static longitudinal stability of the model as the trimmed lift coefficient increased (fig. 6) did not appear to be of great significance in the flight behavior of the model except possibly at the highest lift coefficients. At high lift coefficients there was some indication that the model was not as steady longitudinally as it was at the lower lift coefficients although there was never any indication of static longitudinal instability at angles of attack up to the highest angle ($\alpha_k = 40^{\circ}$). The model was generally easy to fly and, once trim conditions were established, smooth flights of considerable duration were achieved in which little corrective control was required.

Pitching the wing for longitudinal control provided a satisfactory means of controlling the model. When pitch control was applied, both the wing and the platform moved, but in opposite directions. For example, when nose-up pitch control was applied, the initial motions were that the wing pitched nose-up but the platform pitched nose-down. The significant point here is that the platform motion following a control input was initially opposite to that desired and therefore was detrimental to the response of the system. In effect, this result was very much like a lag in motion response following a control input and, as might be expected, was bothersome to the pilot. In the case of a full-scale man-carrying machine, this initial motion of the platform in the wrong direction would be even more bothersome to the pilot because the angular acceleration he would feel following a control input would initially be opposite to that expected.

It was noticed in the flight tests that when the model pitched down to low angles of attack ($\alpha_k = 20^{\circ}$ to 18°) after a stall, or when a disturbance resulted in the model pitching down to this angle-of-attack range, there usually occurred a sudden collapse of the canopy with very little warning from the trailing-edge flutter. Low-aspect-ratio parawings have shown a more gradual change in canopy shape with a decrease in loading as the angle of attack was reduced.

Lateral stability and control.- The lateral stability characteristics of the model were found to be generally satisfactory over the angle-of-attack range. The model was directionally stable and the lateral oscillations were well damped.

Rolling the wing for lateral control was reasonably effective for controlling the model but was considered relatively weak and was consistently rated low in terms of conventional airplane control power requirements. Because of the good stability, however, this relatively weak control was generally satisfactory for maintaining wing-level flight and for performing the mild maneuvers possible in the tunnel. This result is in contrast to the flight result obtained previously with low-aspect-ratio parawings (refs. 4 and 5), where it was found that the wing-bank control system was completely ineffective for

lateral control at high angles of attack. This difference in control between the two wings is believed to be associated primarily with the higher directional stability and lower effective dihedral obtained with the higher aspect ratio wing.

The control provided by wing bank seemed to be most effective at keel angles of attack near 28° to 30°, and an increase from this angle resulted in a progressive decrease in control effectiveness. The deterioration in control at the higher angles of attack is probably associated mainly with adverse yawing moments inherent in the wing bank system and with the reduction in directional stability of the configuration. (See figs. 8 to 13.)

As in the case of the longitudinal control, when roll control was applied, both the wing and the platform tilted, but in opposite directions. For example, when right roll control was applied, the initial motions were that the wing was banked to the right, but the platform was banked to the left. This initial motion of the platform in the wrong direction following control input was more bothersome to the pilot than was the case for longitudinal control because the initial motion of the body in a direction opposite to that desired following the control input was much more pronounced than that for the longitudinal case. Once the pilot became adjusted to this type of motion, however, fairly smooth flights could be made with little attention to control.

This problem of relative motion between the body and wing would probably be more bothersome to the pilot of the full-scale airplane because the angular acceleration he would feel following a control input would initially be opposite to that expected. This result and the fact that the lateral stick forces are inherently high in a vehicle of this type are factors which would undoubtedly adversely affect the pilot's rating of the flying qualities of the vehicle.

The use of rudder coordinated with wing bank for lateral control provided satisfactory lateral control over the entire test angle-of-attack range. As in the case of other parawing utility vehicles, the rudder alone provided generally satisfactory lateral control characteristics at the higher angles of attack. The rudder provides roll control in an indirect manner by sideslipping the model and making use of the positive dihedral effect to cause roll. At the higher angles of attack (above about 35°) the rudder alone provided better lateral control than that provided by wing bank alone. At the lower angles of attack, down to the lowest angle of attack flown $(\alpha_k = 23^{\circ})$, the response of the model to rudder was found to decrease (probably because of a reduction in dihedral effect) but, despite this fact, it was still felt that the rudder provided satisfactory lateral control and was about as effective for roll control as the wing bank system in this angle-of-attack range.

CONCLUDING REMARKS

Although neither stick forces nor the effects of flexibility were taken into account in the present investigation, it is believed that the results of the investigation provide a qualitative indication of the overall flight characteristics of a parawing vehicle of this type.

The model had satisfactory dynamic longitudinal and lateral stability and the motions were well damped over the angle-of-attack range (keel angles of 23° to 40°). The stability and control characteristics of the present model with the aspect-ratio-6 conical parawing were generally more satisfactory than those of the same model with an aspect-ratio-3 conical parawing which had previously been investigated.

The center-of-gravity-shift control system was reasonably effective for controlling the model but was considered to be relatively weak and was consistently rated low in terms of conventional airplane control power requirements. Because of the good stability, however, this relatively weak control was generally satisfactory for maintaining wing-level flight and for performing the mild maneuvers possible in the tunnel.

The rudder alone was about as effective for lateral control as the wing-bank system at low and moderate angles of attack and provided better control than the wing-bank system at the higher angles of attack (above about 35°).

The most satisfactory control was obtained when the rudder was coordinated with the wing-bank control.

Langley Research Center,
National Aeronautics and Space Administration,
Langley Station, Hampton, Va., August 24, 1966,
126-13-01-19-23.

REFERENCES

1. Polhamus, Edward C.; and Naeseth, Rodger L.: Experimental and Theoretical Studies of the Effects of Camber and Twist on the Aerodynamic Characteristics of Parawings Having Nominal Aspect Ratios of 3 and 6. NASA TN D-972, 1963.

2. Bugg, Frank M.: Effects of Aspect Ratio and Canopy Shape on Low-Speed Aerodynamic Characteristics of 50.0° Swept Parawings. NASA TN D-2922, 1965.

3. Sleeman, William C., Jr.; and Johnson, Joseph L., Jr.: Parawing Aerodynamics. Astronautics and Aerospace Eng., vol. 1, no. 5, June 1963, pp. 49-55.

4. Johnson, Joseph L., Jr.: Low-Speed Force and Flight Investigation of a Model of a Modified Parawing Utility Vehicle. NASA TN D-2492, 1965.

5. Johnson, Joseph L., Jr.: Low-Speed Wind-Tunnel Investigation To Determine the Flight Characteristics of a Model of a Parawing Utility Vehicle. NASA TN D-1255, 1962.

6. Mechtly, E. A.: The International System of Units – Physical Constants and Conversion Factors. NASA SP-7012, 1964.

7. Paulson, John W.; and Shanks, Robert E.: Investigation of Low-Subsonic Flight Characteristics of a Model of a Hypersonic Boost-Glide Configuration Having a 78° Delta Wing. NASA TN D-894, 1961. (Supersedes NASA TM X-201.)

8. Johnson, Joseph L., Jr.; and Hassell, James L., Jr.: Full-Scale Wind-Tunnel Investigation of a Flexible-Wing Manned Test Vehicle. NASA TN D-1946, 1963.

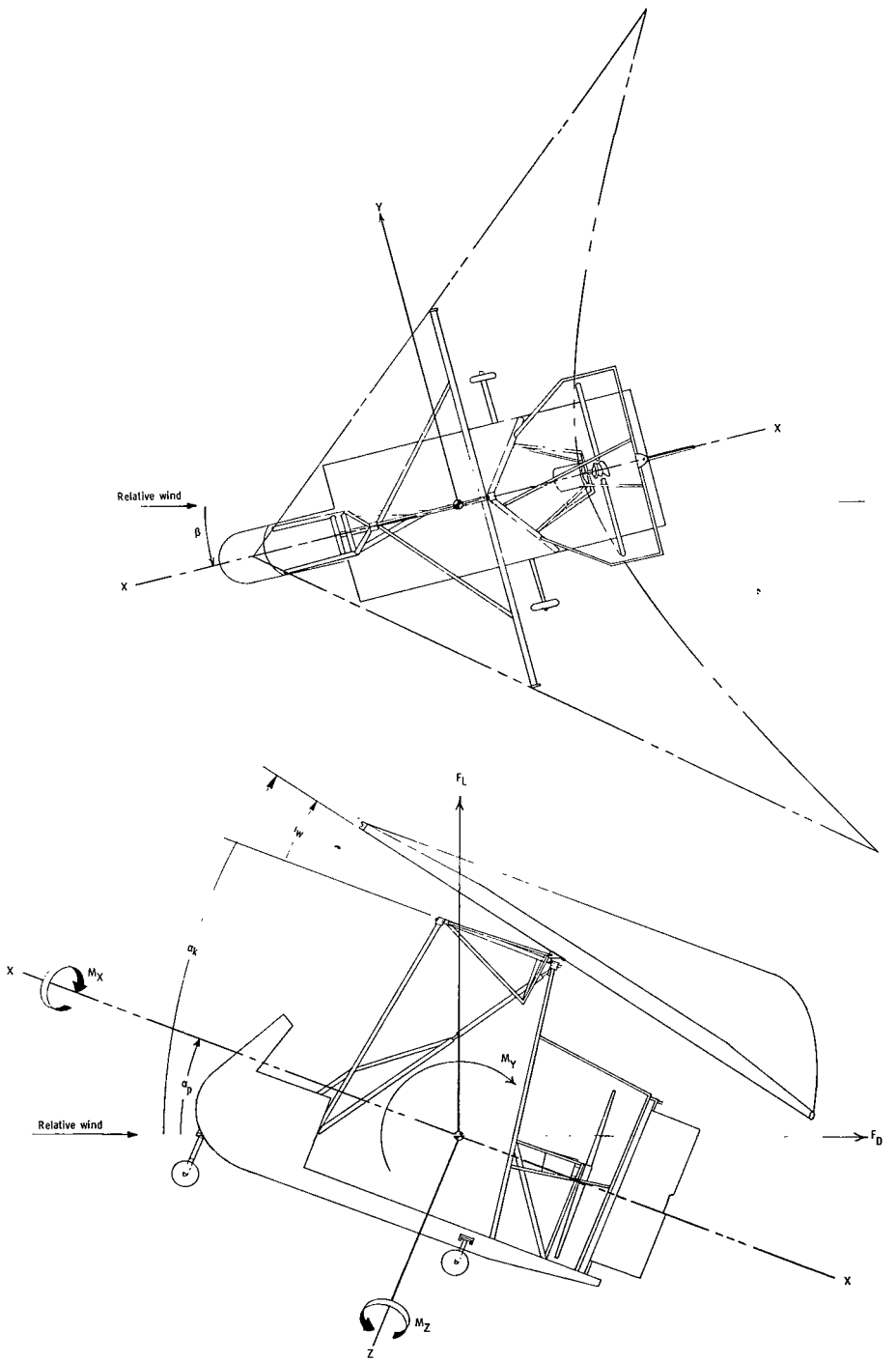

Figure 1.- System of axes used in investigation. Longitudinal data are referred to wind axes and lateral data are referred to body axes unless otherwise noted. Arrows indicate positive direction of forces, moments, and angles.

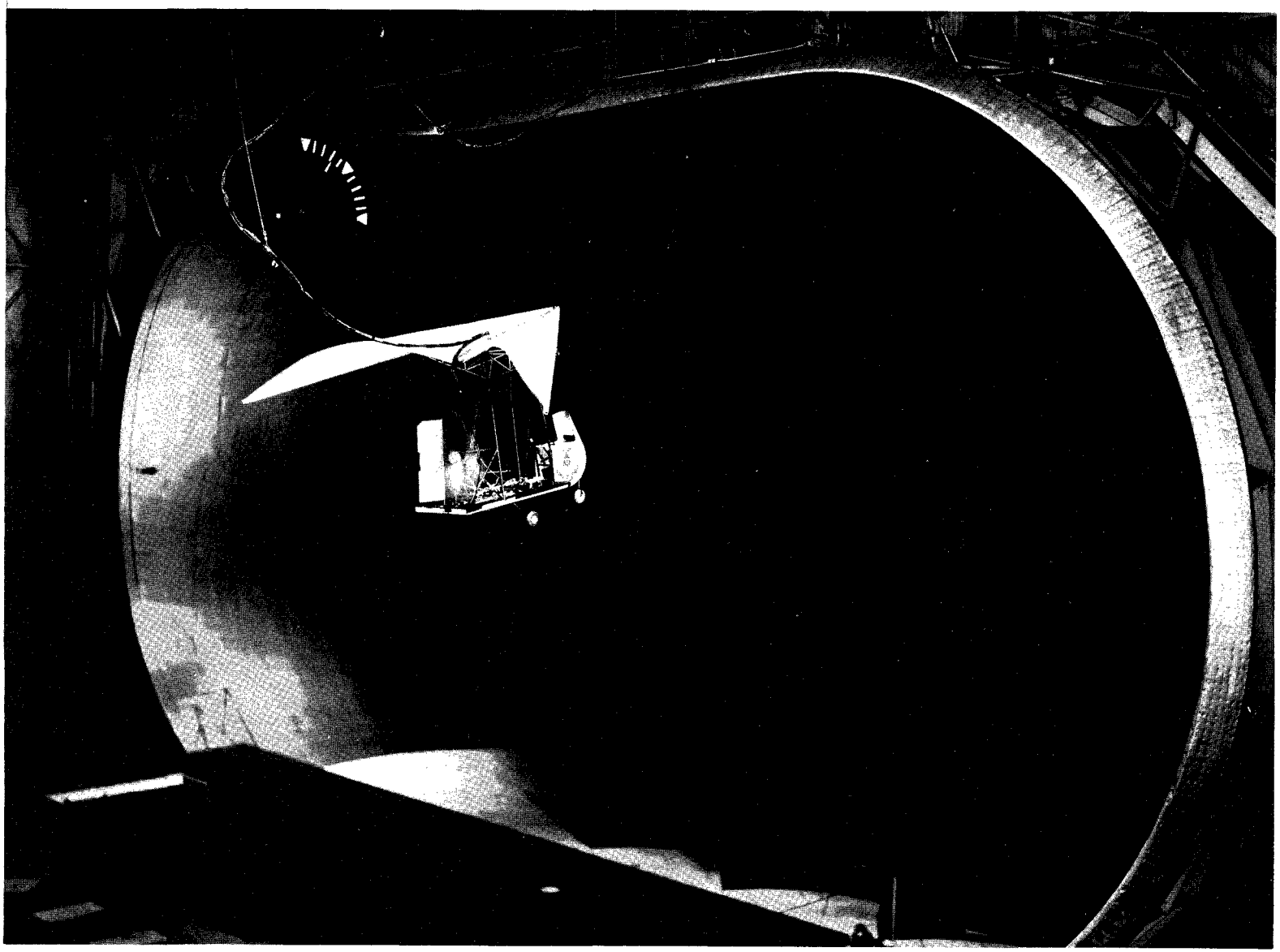

Figure 2.- Three-quarter rear view of the model flying in the Langley full-scale tunnel. L-65-2576

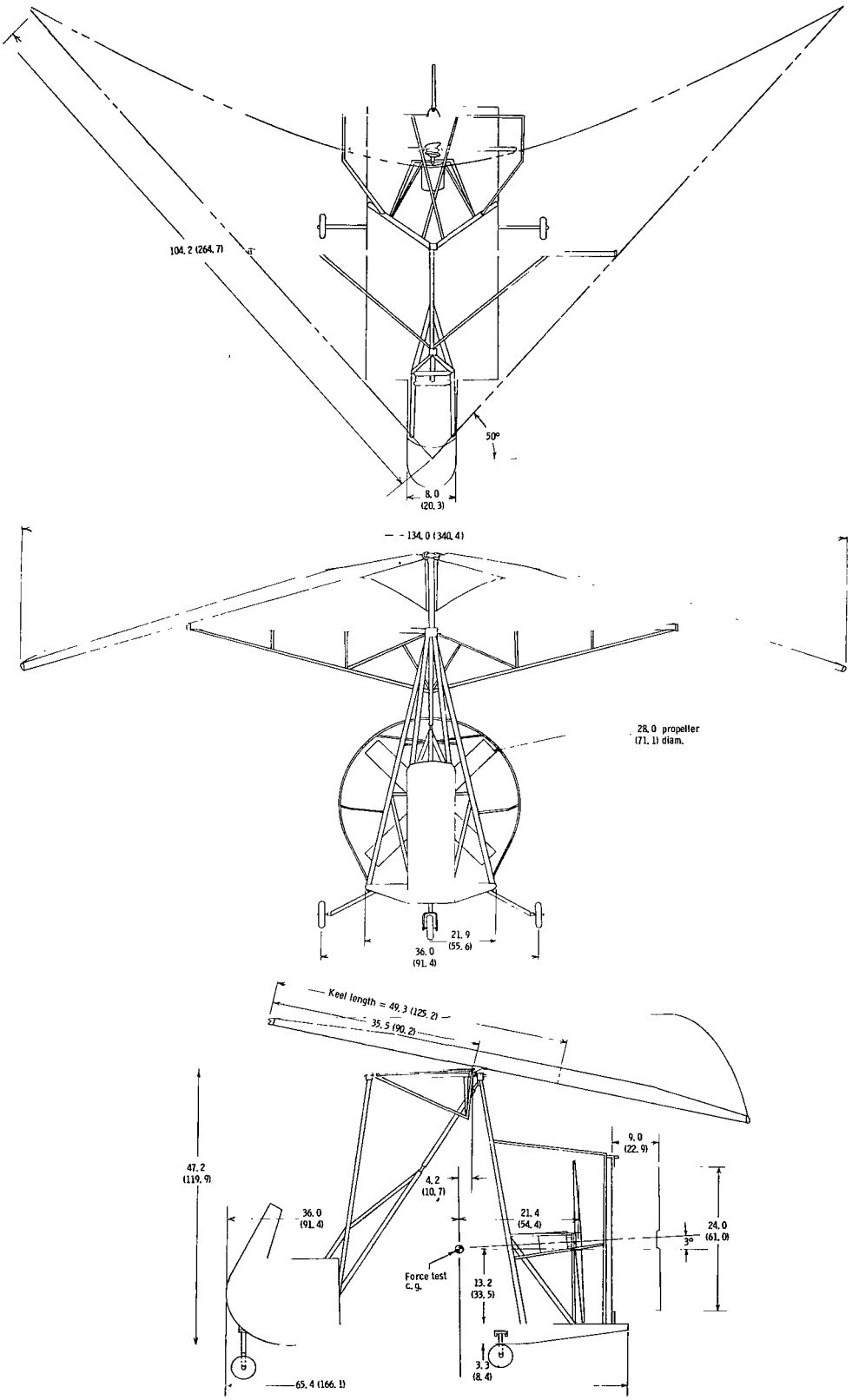

Figure 3.- Three-view drawing of model used in investigation. All dimensions are in inches with centimeters given in parentheses.

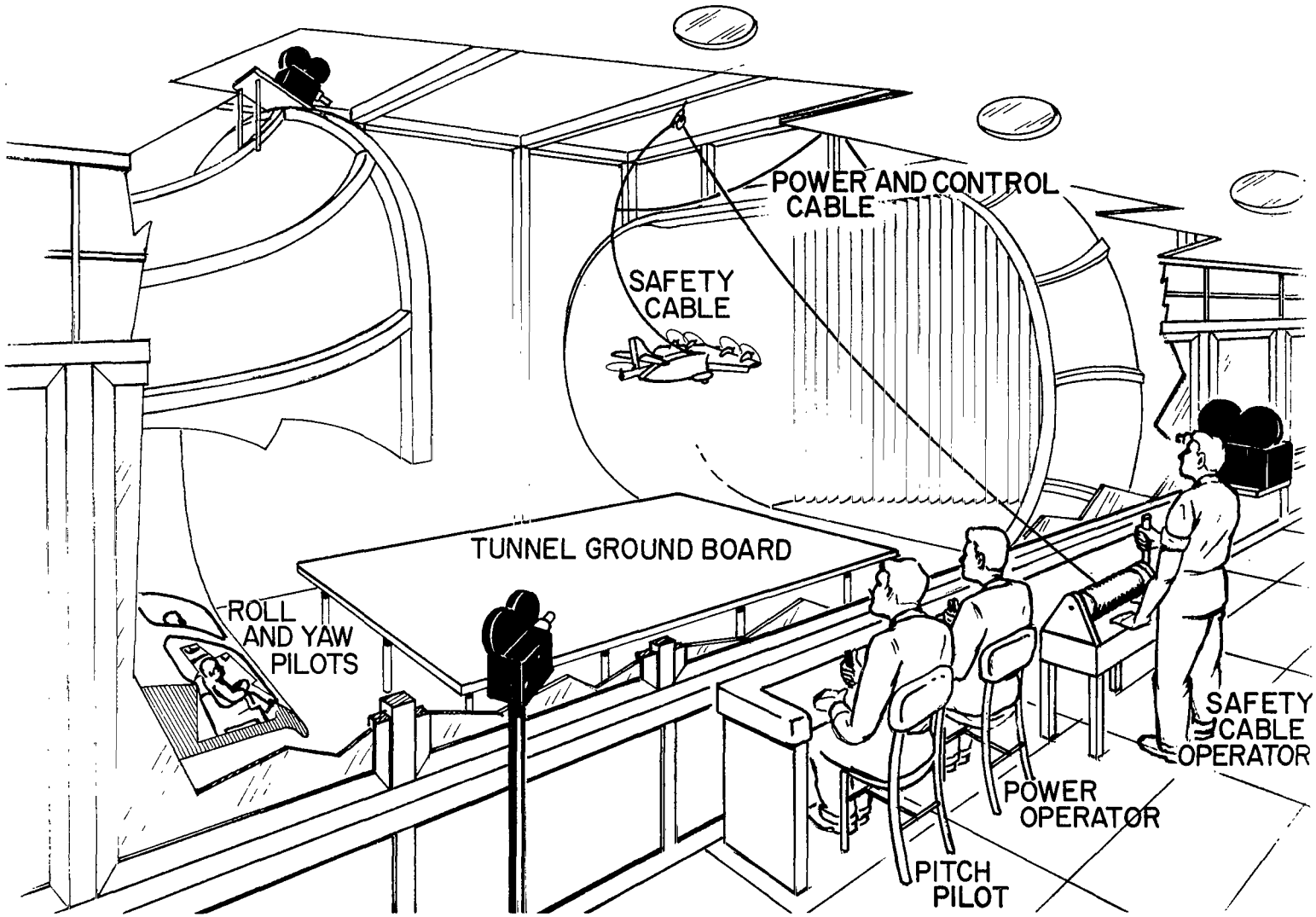

Figure 4.- Setup for flight tests in the Langley full-scale tunnel. L-64-3008

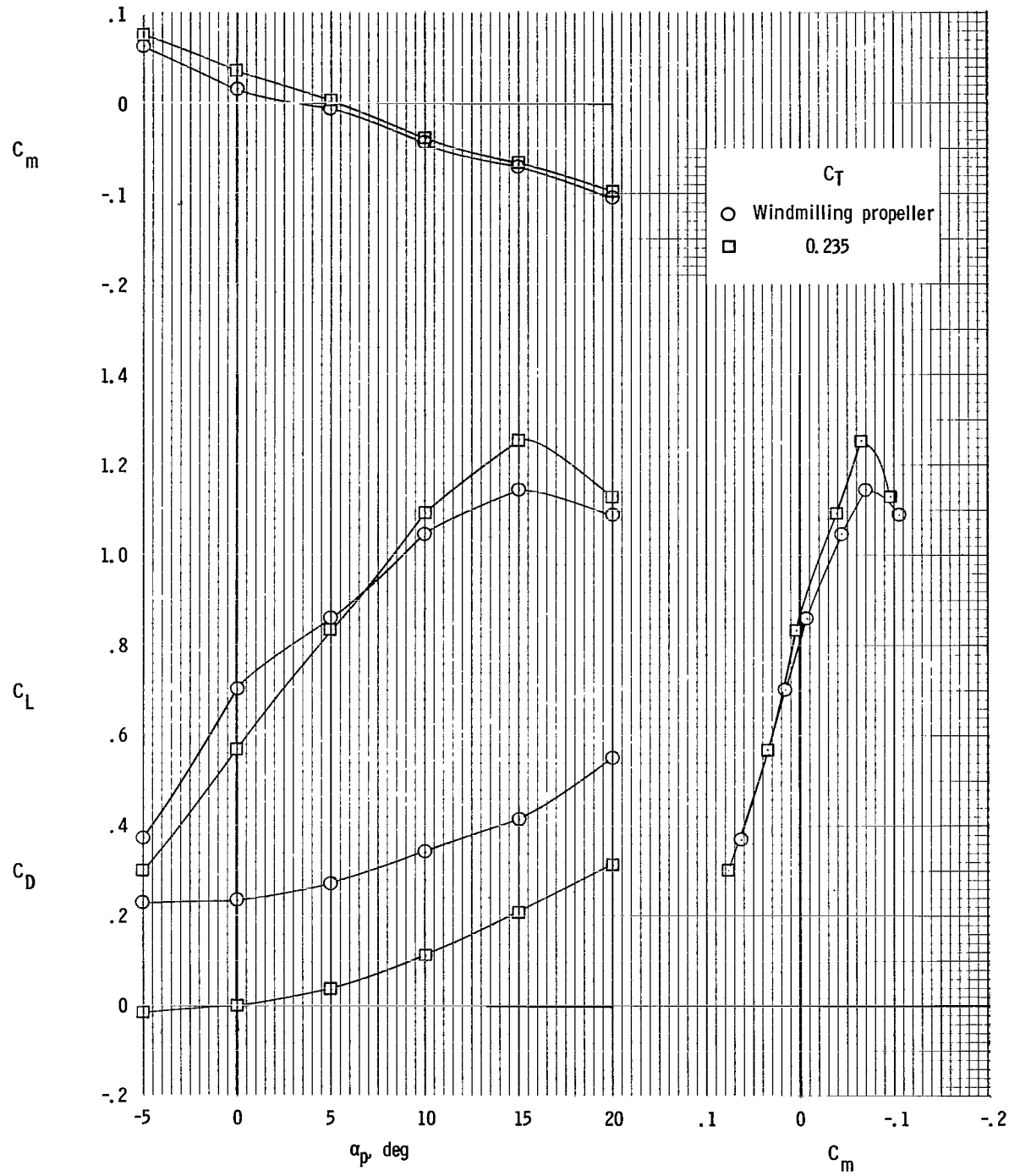

(a) $i_w = 20^0$.

Figure 5.- Static longitudinal characteristics of model. $\beta = 0^0$.

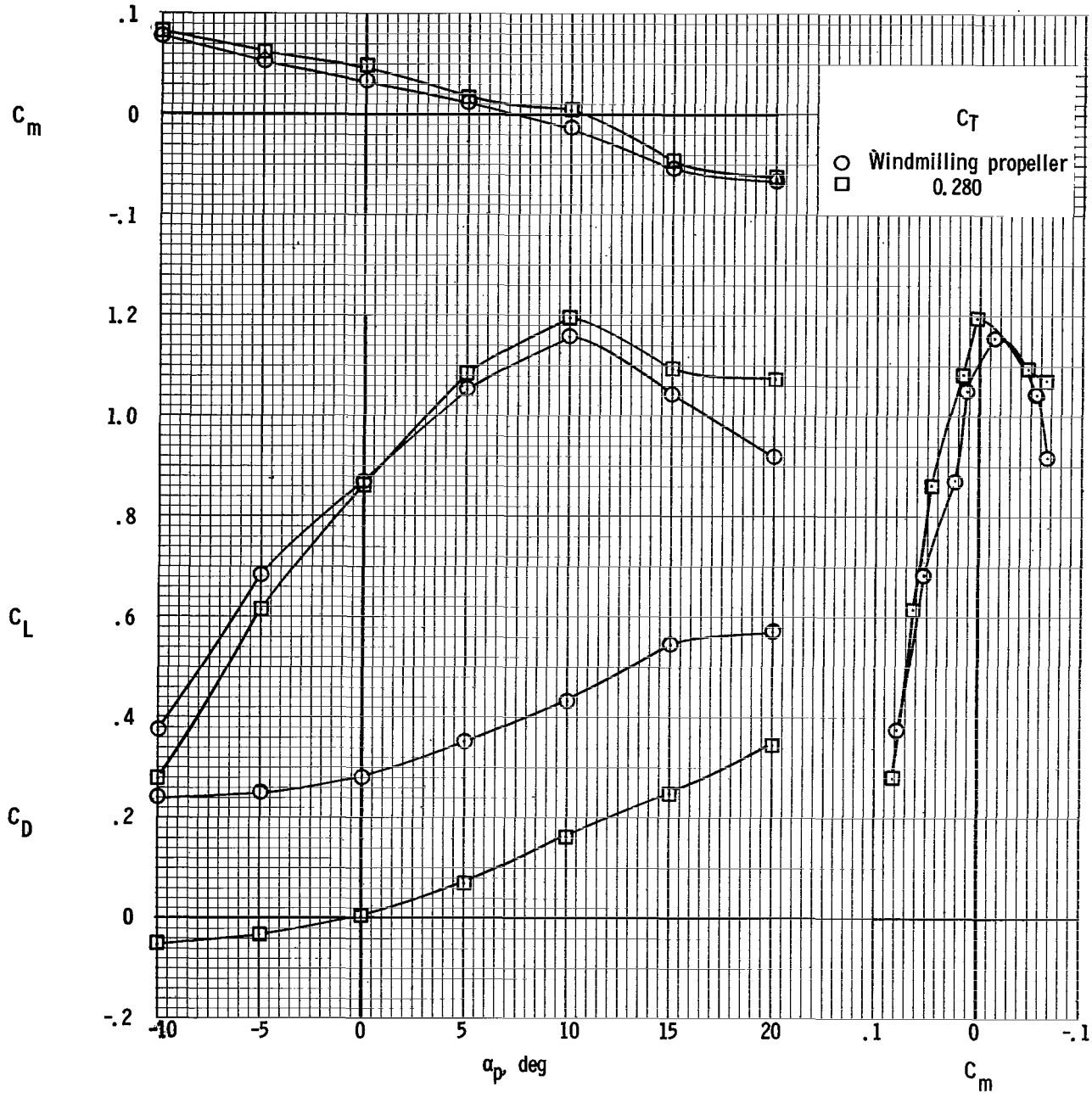

(b) $i_w = 25^0$.

Figure 5.- Continued.

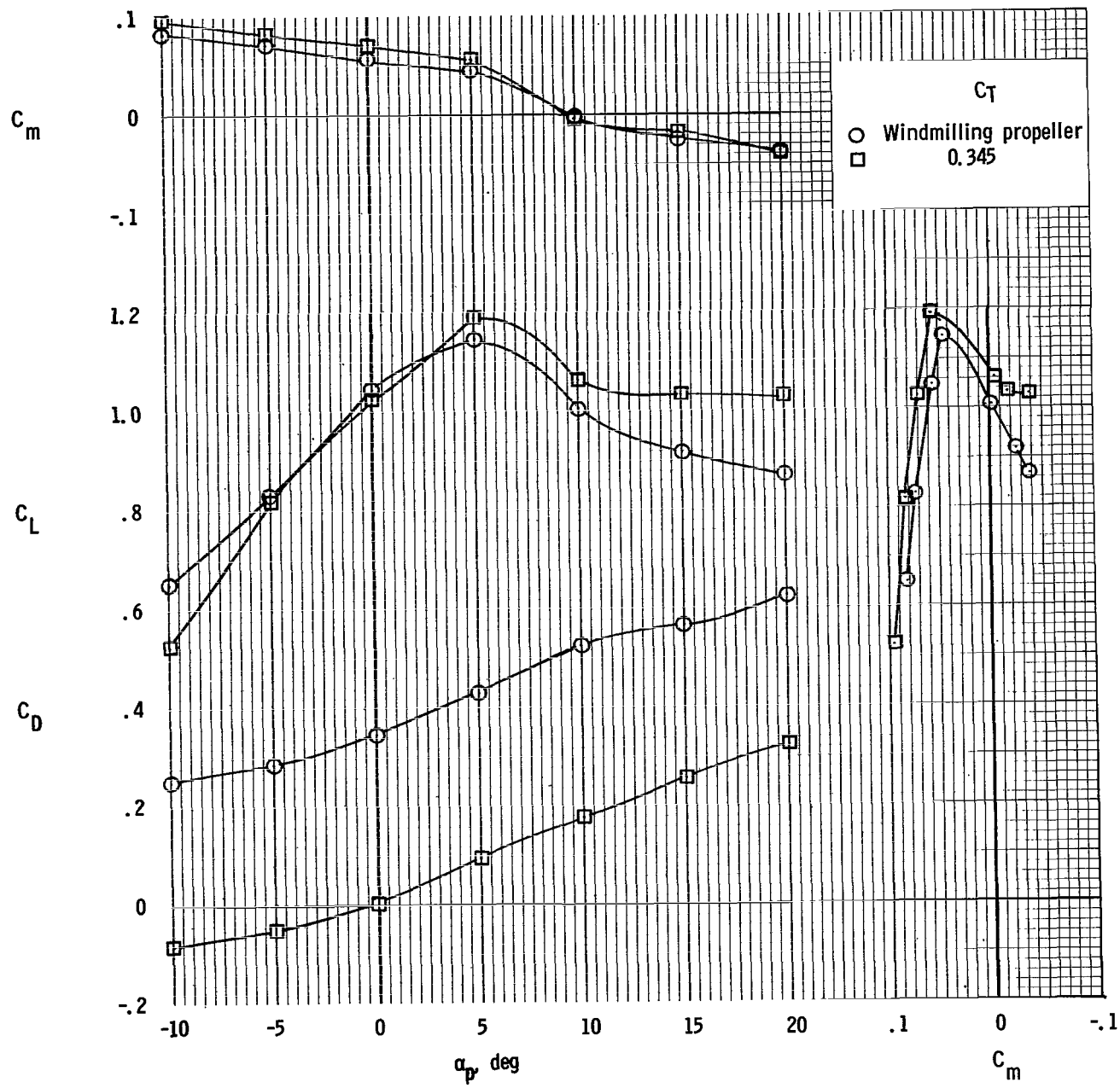

(c) $i_w = 30^o$.

Figure 5.- Concluded.

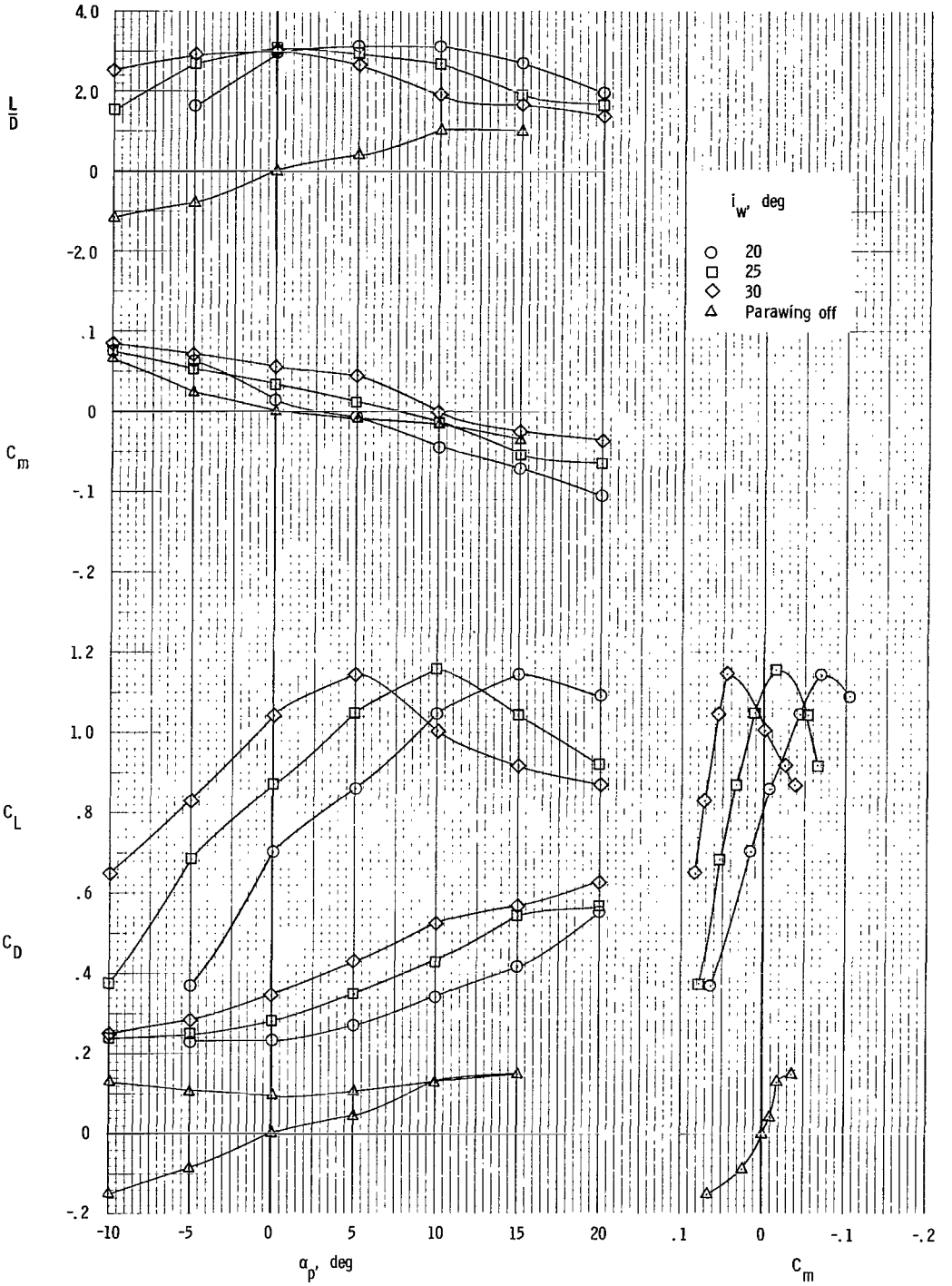

(a) Data presented about platform angle.

Figure 6.- Summary of static longitudinal characteristics of model. Windmilling propeller. $\beta = 0^{o}$.

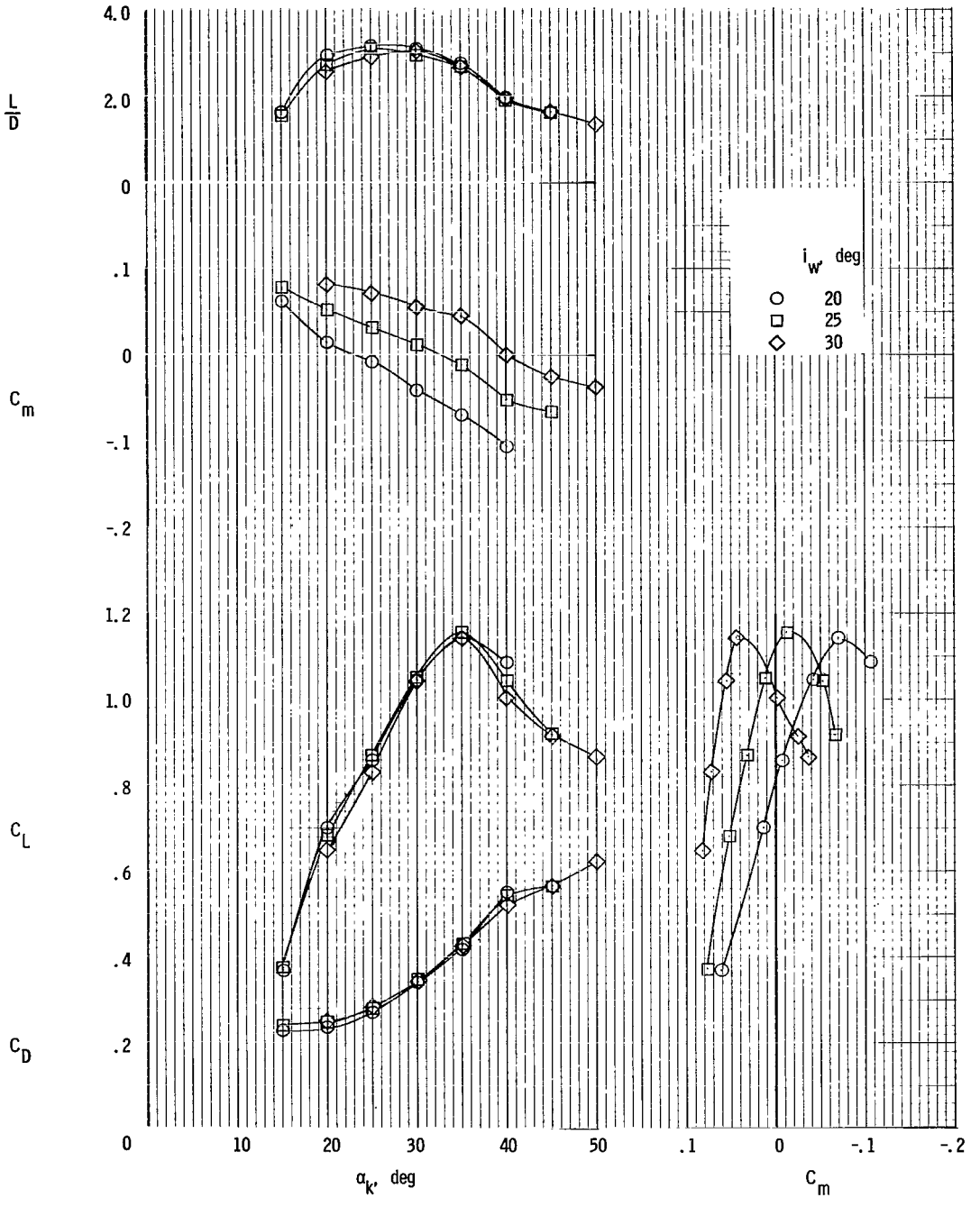

(b) Data presented about keel angle.

Figure 6.- Concluded.

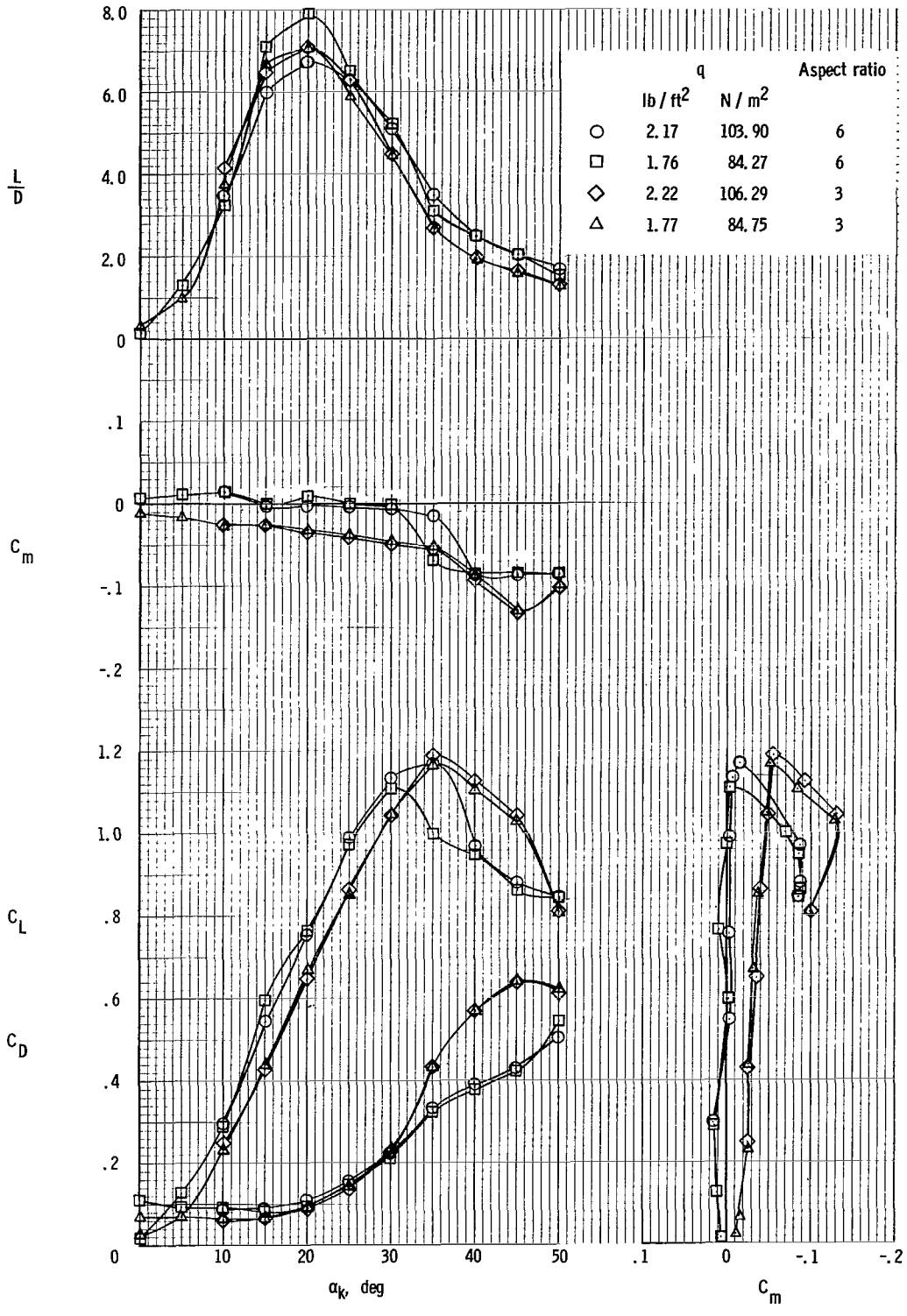

Figure 7.- Static longitudinal characteristics of parawing alone. $\beta = 0^{o}$. (Moment center located at wing pivot.)

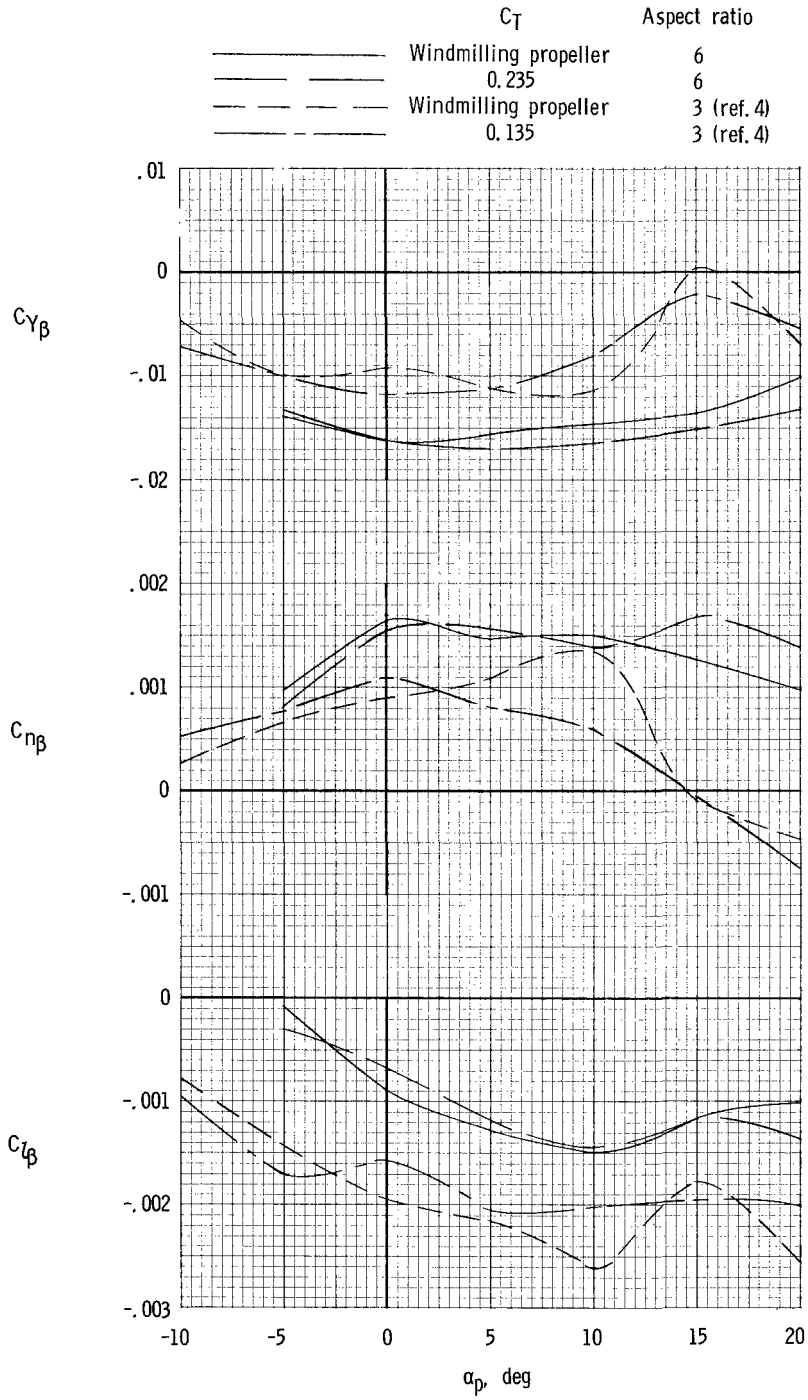

(a) $i_w = 20^o$.

Figure 8.- Variation of the static lateral stability characteristics of the model with angle of sideslip for the power-on and windmilling propeller conditions.

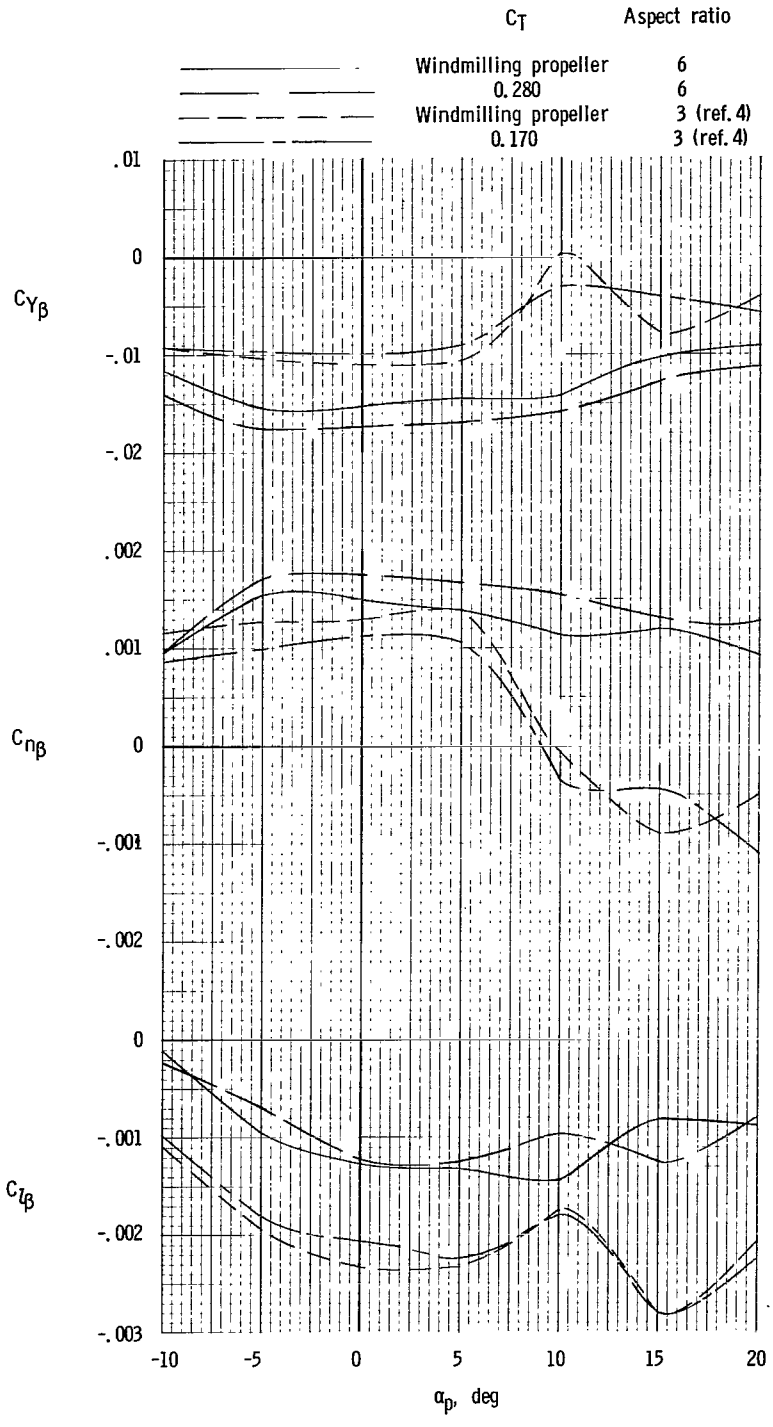

(b) $i_w = 25^0$.

Figure 8.- Continued.

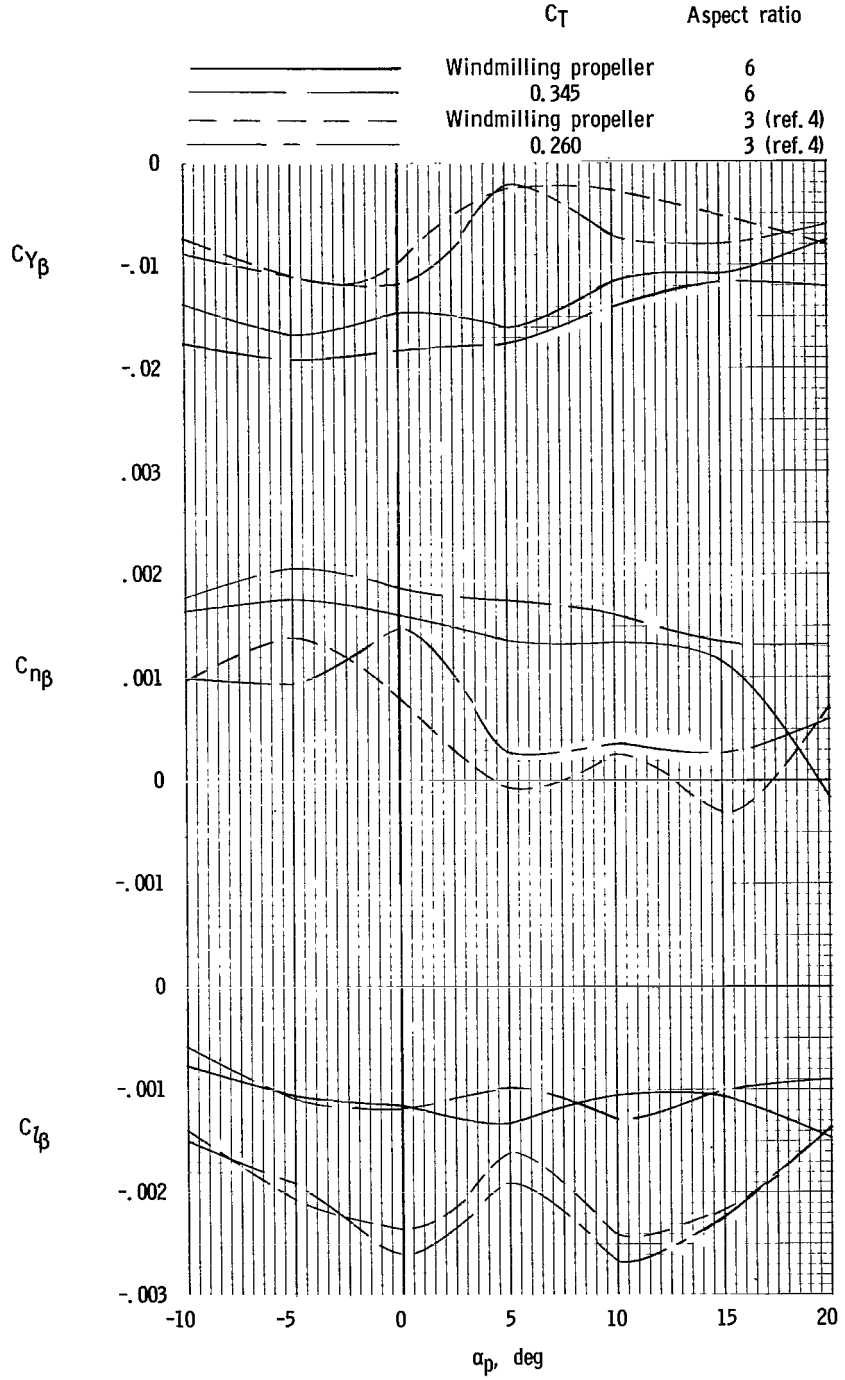

(c) $i_w = 30^0$.

Figure 8.- Concluded.

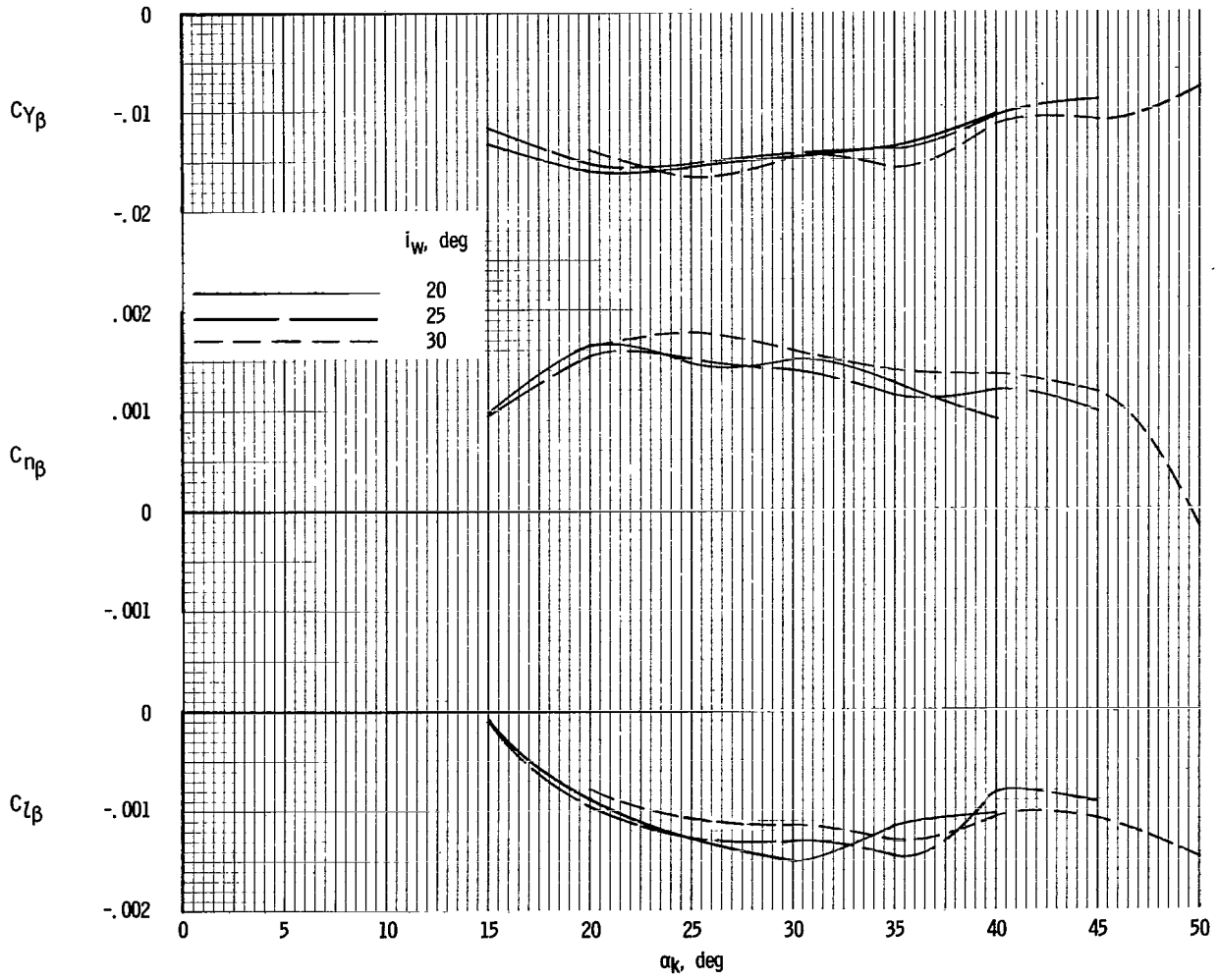

Figure 9.- Variation of lateral stability parameters with keel angle of attack of the parawing model. Windmilling propeller.

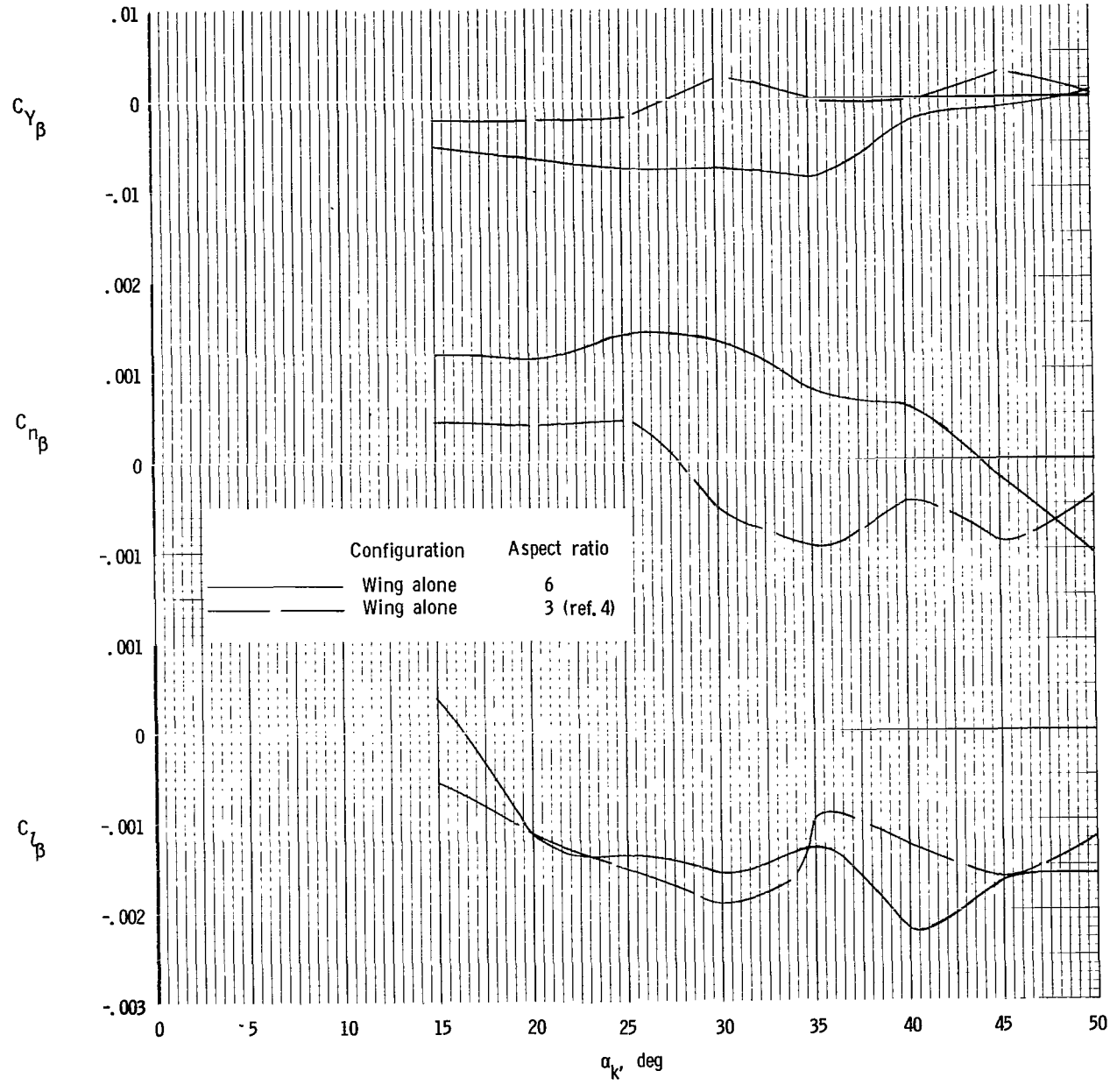

Figure 10.- Static lateral characteristics of the parawings alone for the aspect-ratio-6 and -3 wings. (Data presented about a body system of axes parallel to the parawing keel and originating at the wing pivot point.)

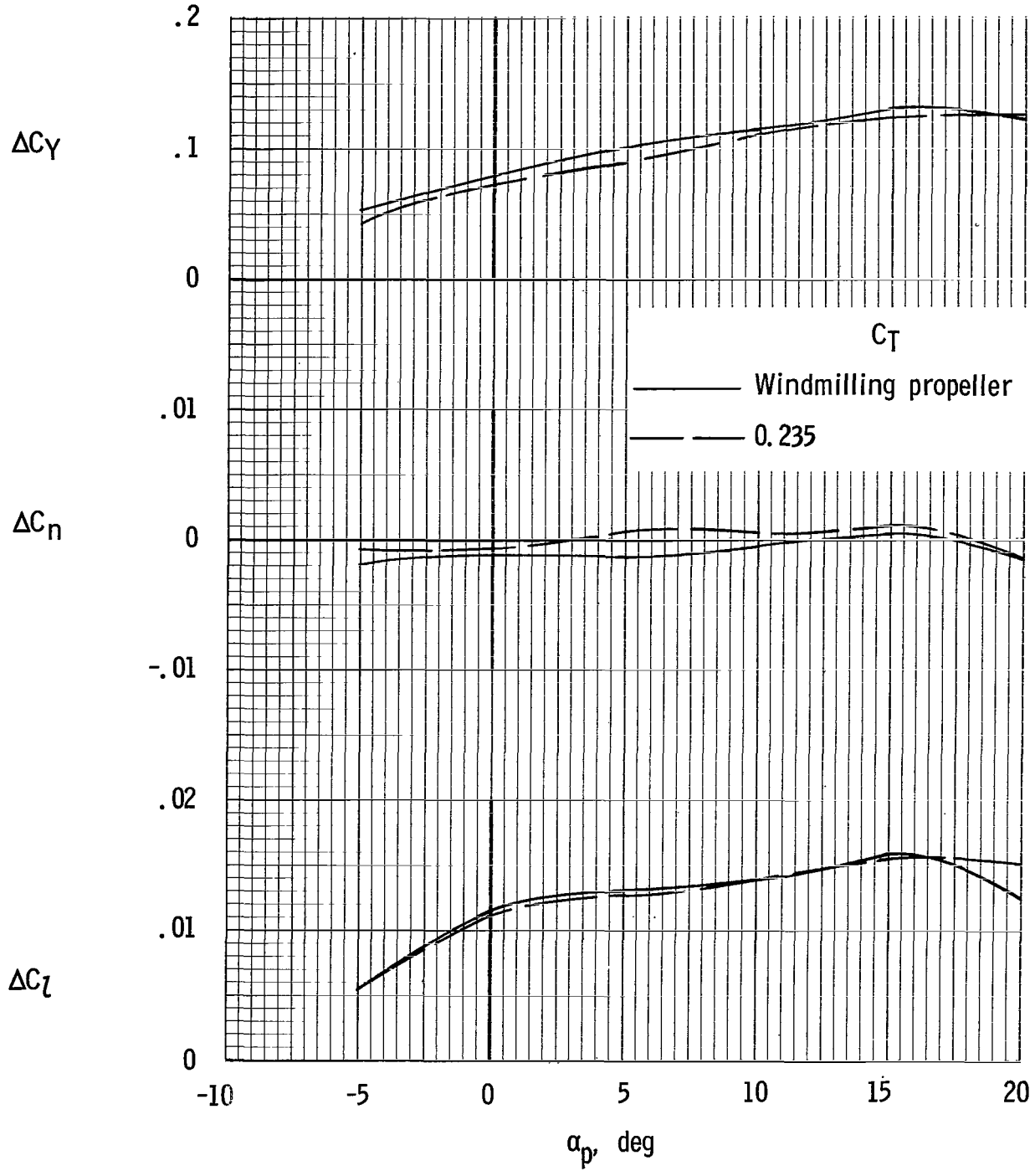

(a) $i_w = 20^0$.

Figure 11.- Incremental lateral forces and moments produced by banking the wing. $\Phi = 5^0$; $\beta = 0^0$.

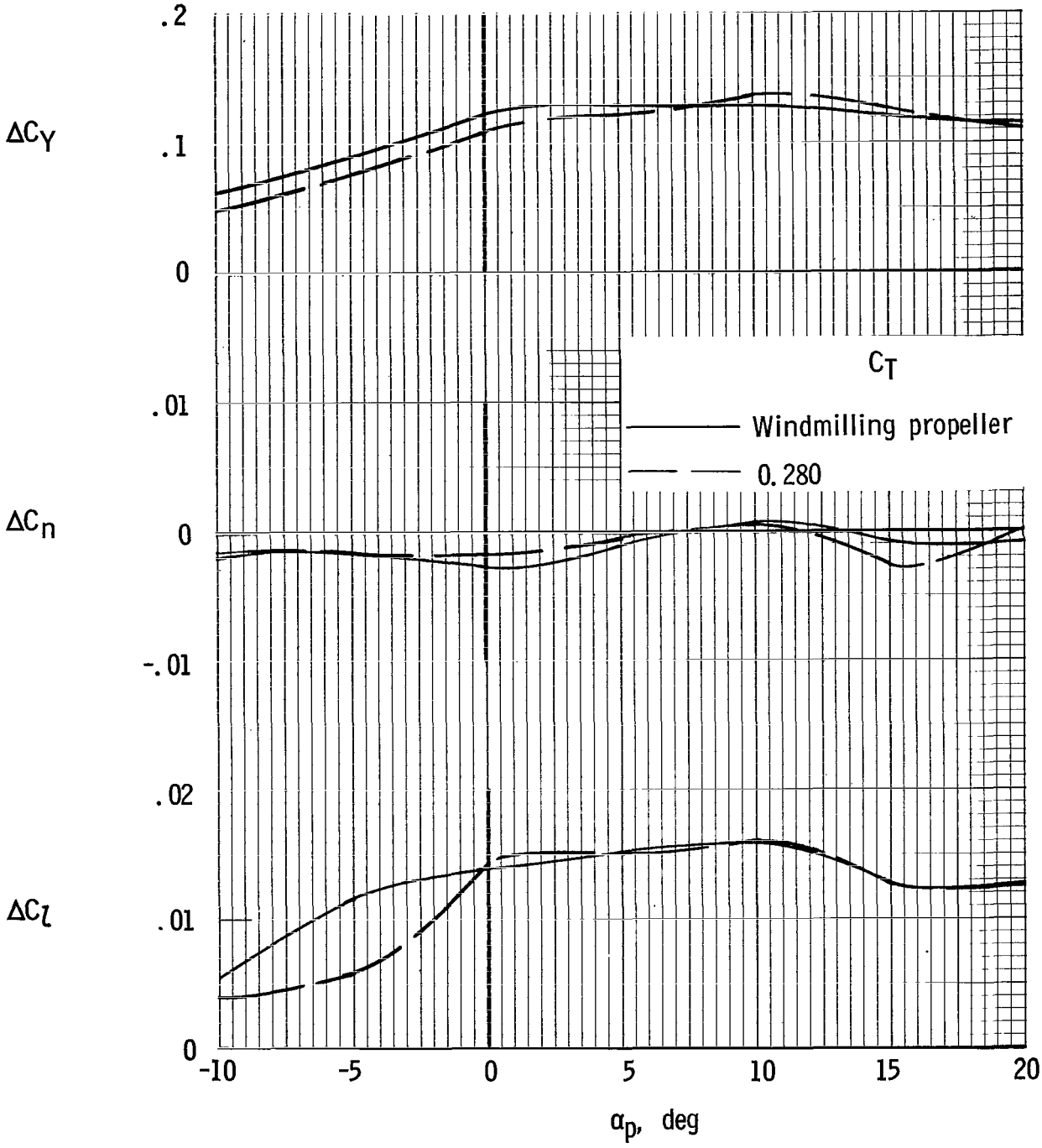

(b) $i_w = 25^o$.

Figure 11.- Continued.

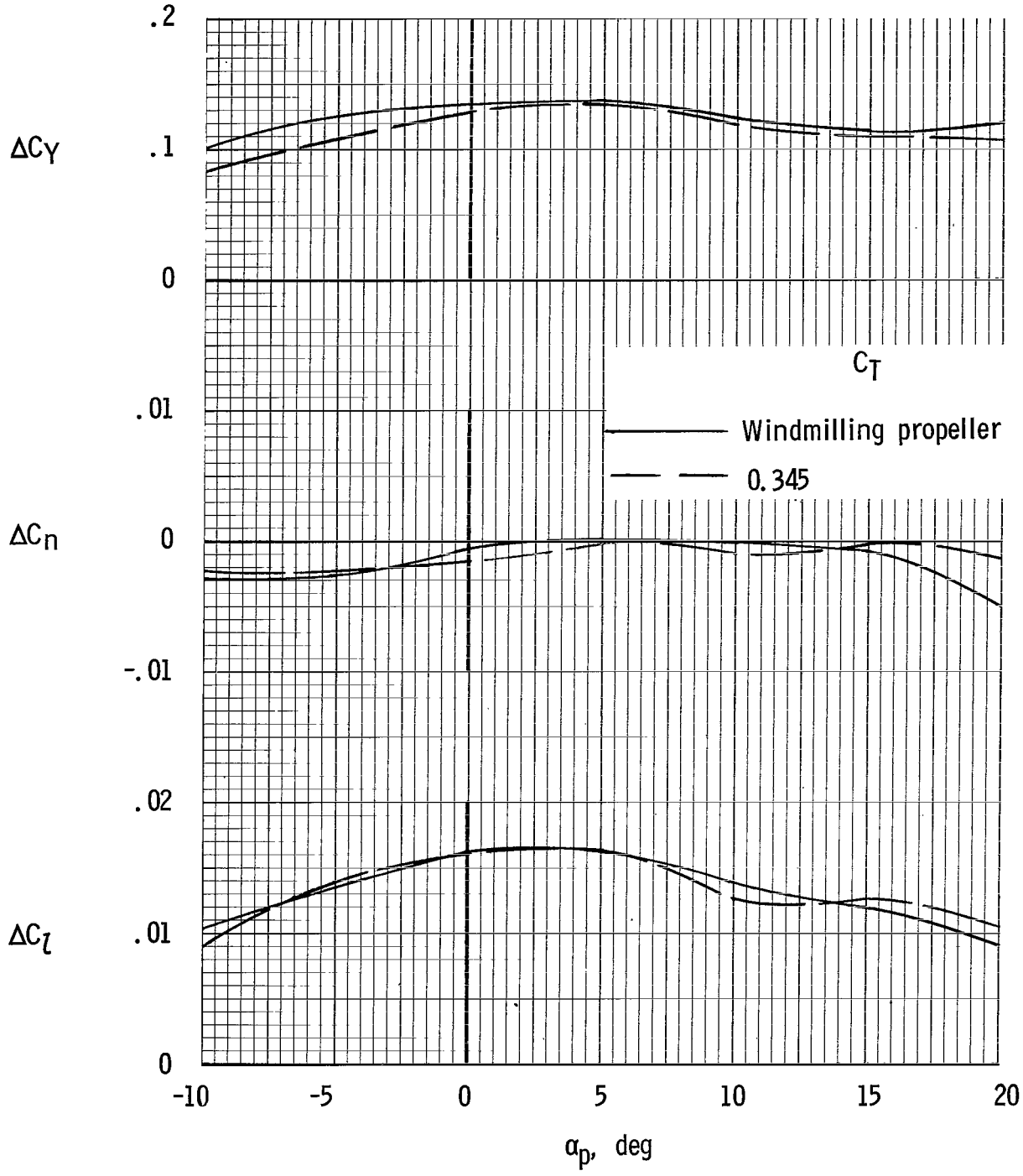

(c) $i_w = 30^0$.

Figure 11.- Concluded.

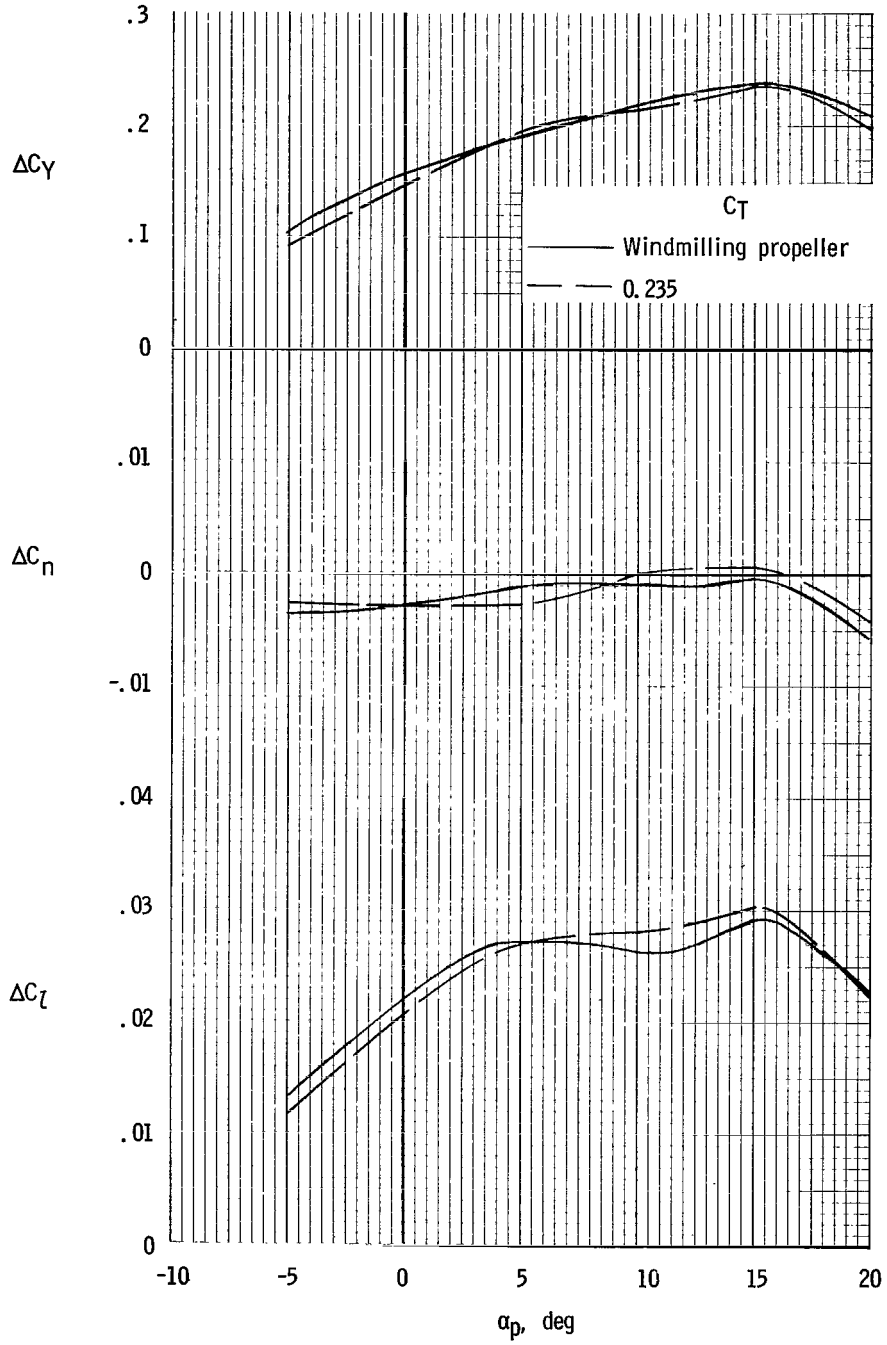

(a) $i_w = 20^0$.

Figure 12.- Incremental lateral forces and moments produced by banking the wing. $\Phi = 10^0$; $\beta = 0^0$.

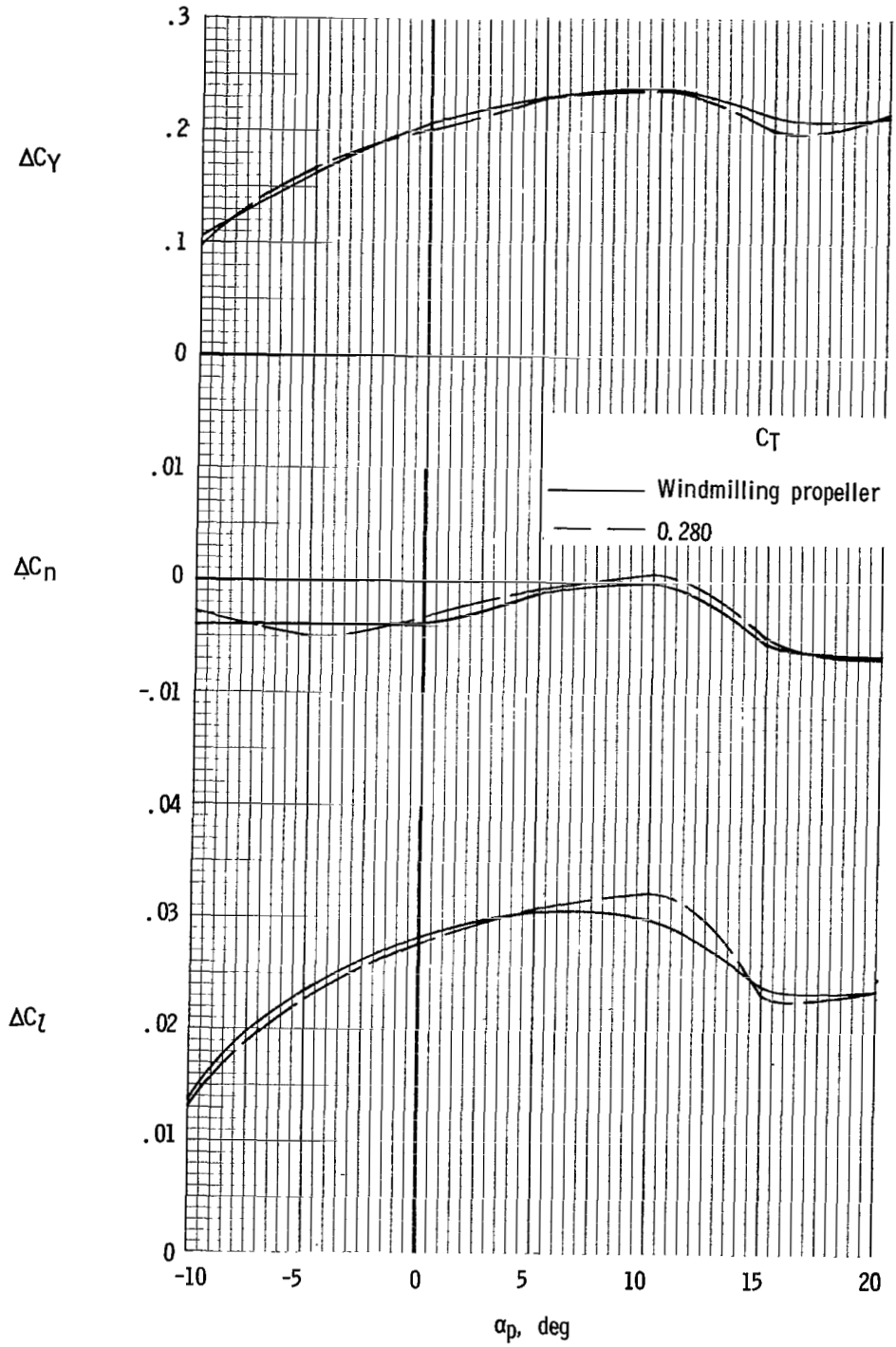

(b) $i_w = 25^0$.

Figure 12.- Continued.

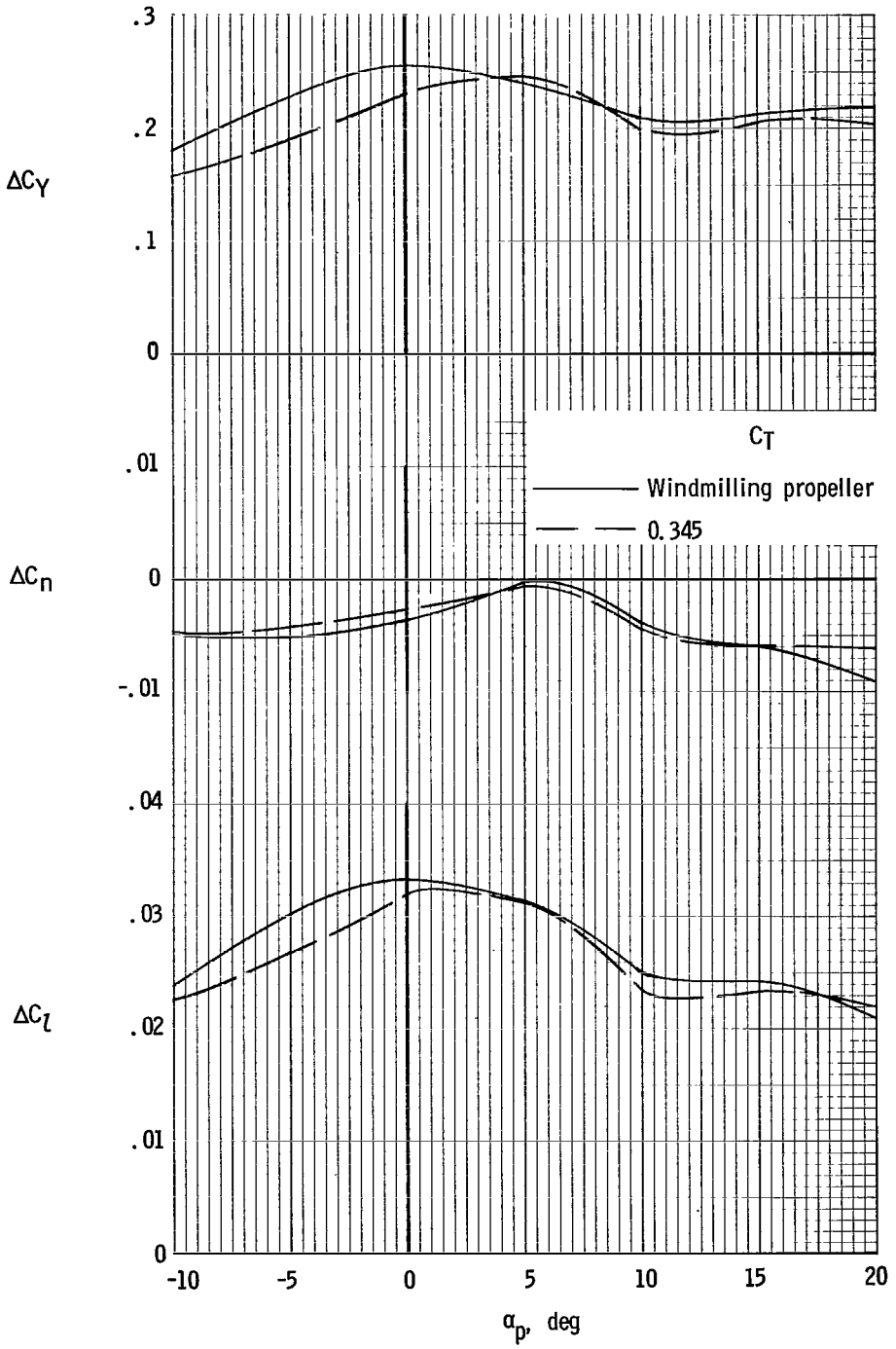

(c) $i_w = 30^o$.

Figure 12.- Concluded.

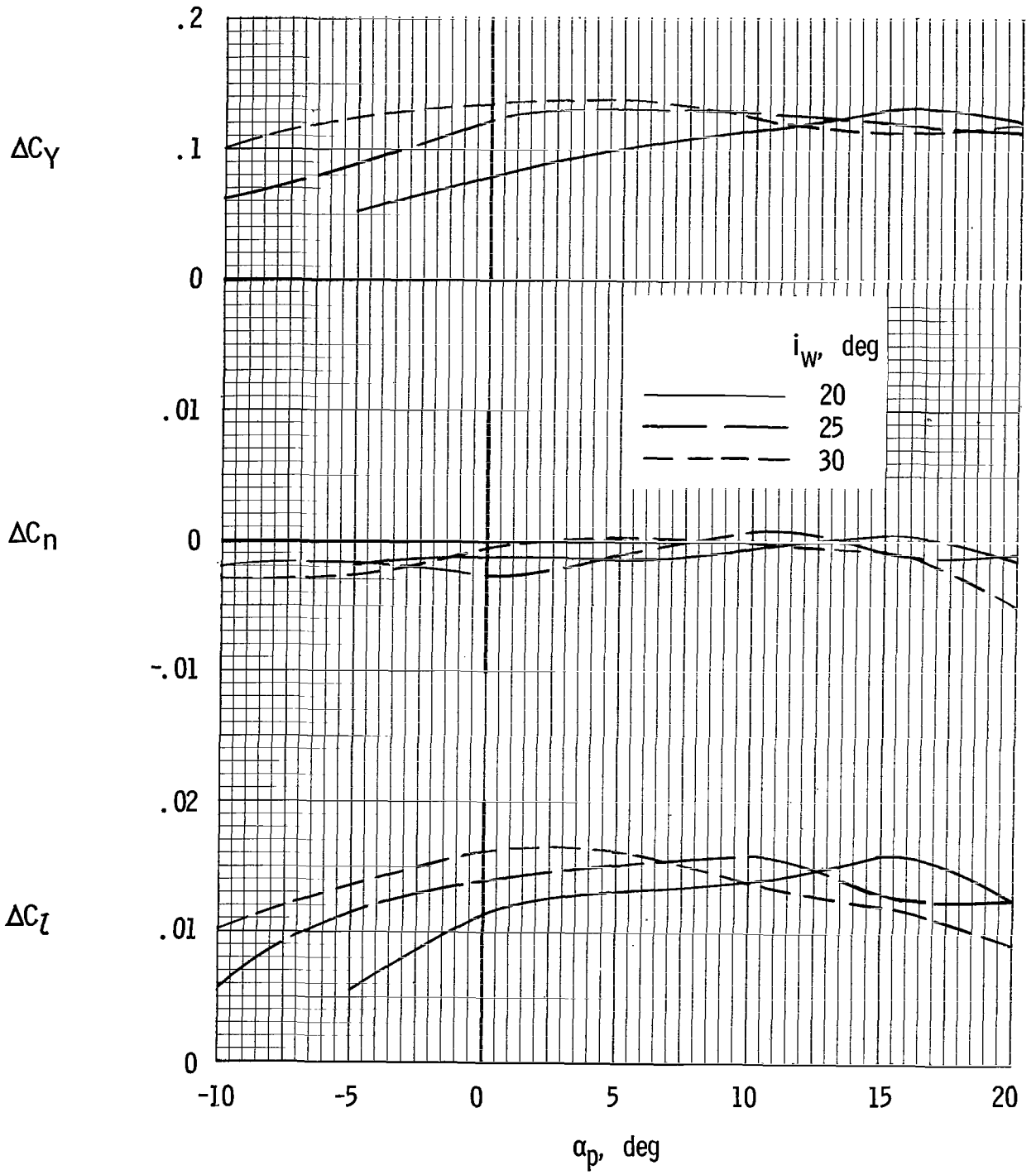

(a) $\Phi = 5^0$.

Figure 13.- Effect of wing incidence on the incremental lateral forces and moments produced by banking the wing.

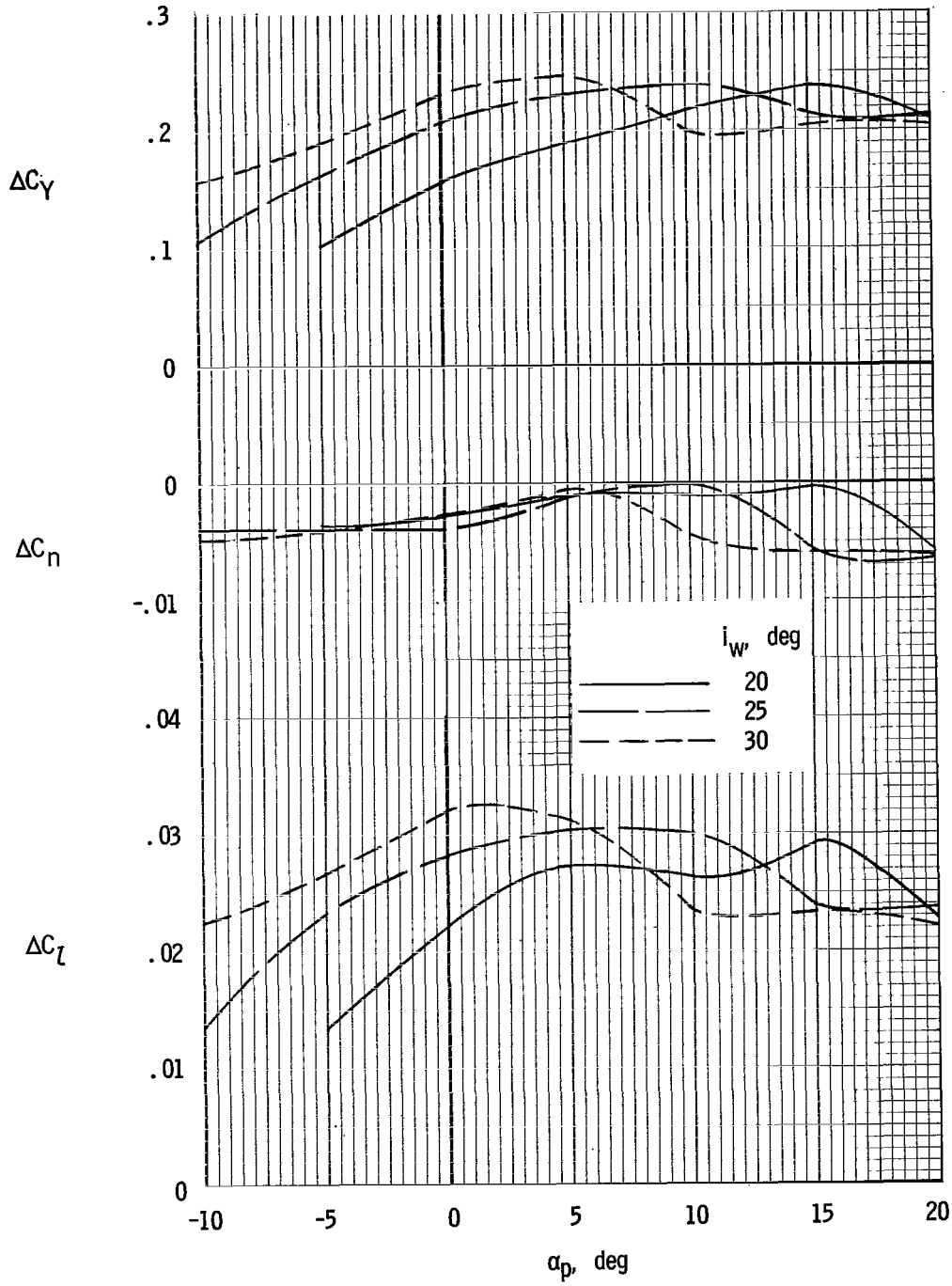

(b) $\Phi = 10^0$.

Figure 13.- Concluded.

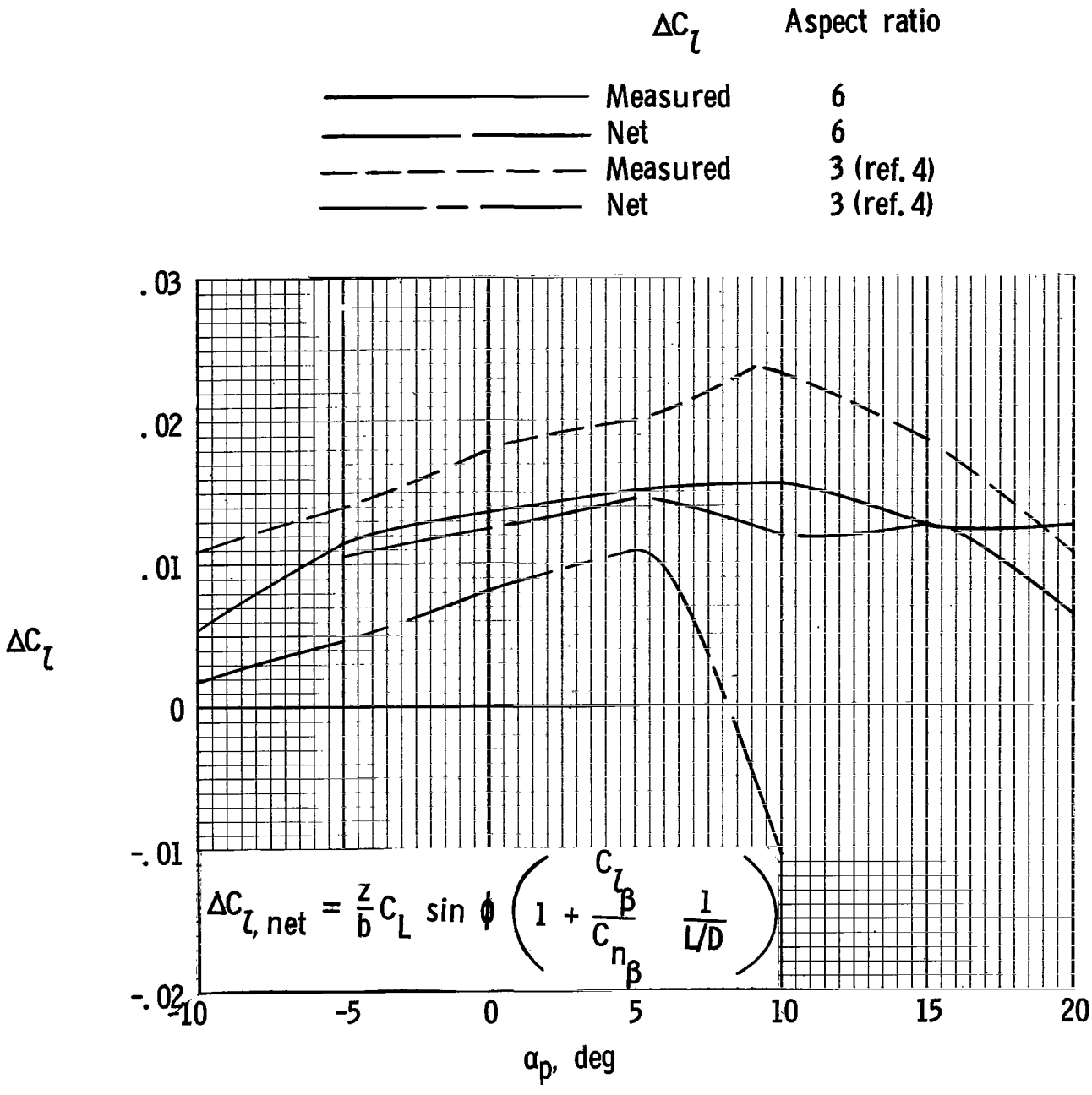

Figure 14.- Comparison of measured rolling moment and calculated net rolling moment produced by banking the wing. (Data referred to stability axis.) Windmilling propeller; $i_w = 25^0$; $\Phi = 5^0$.

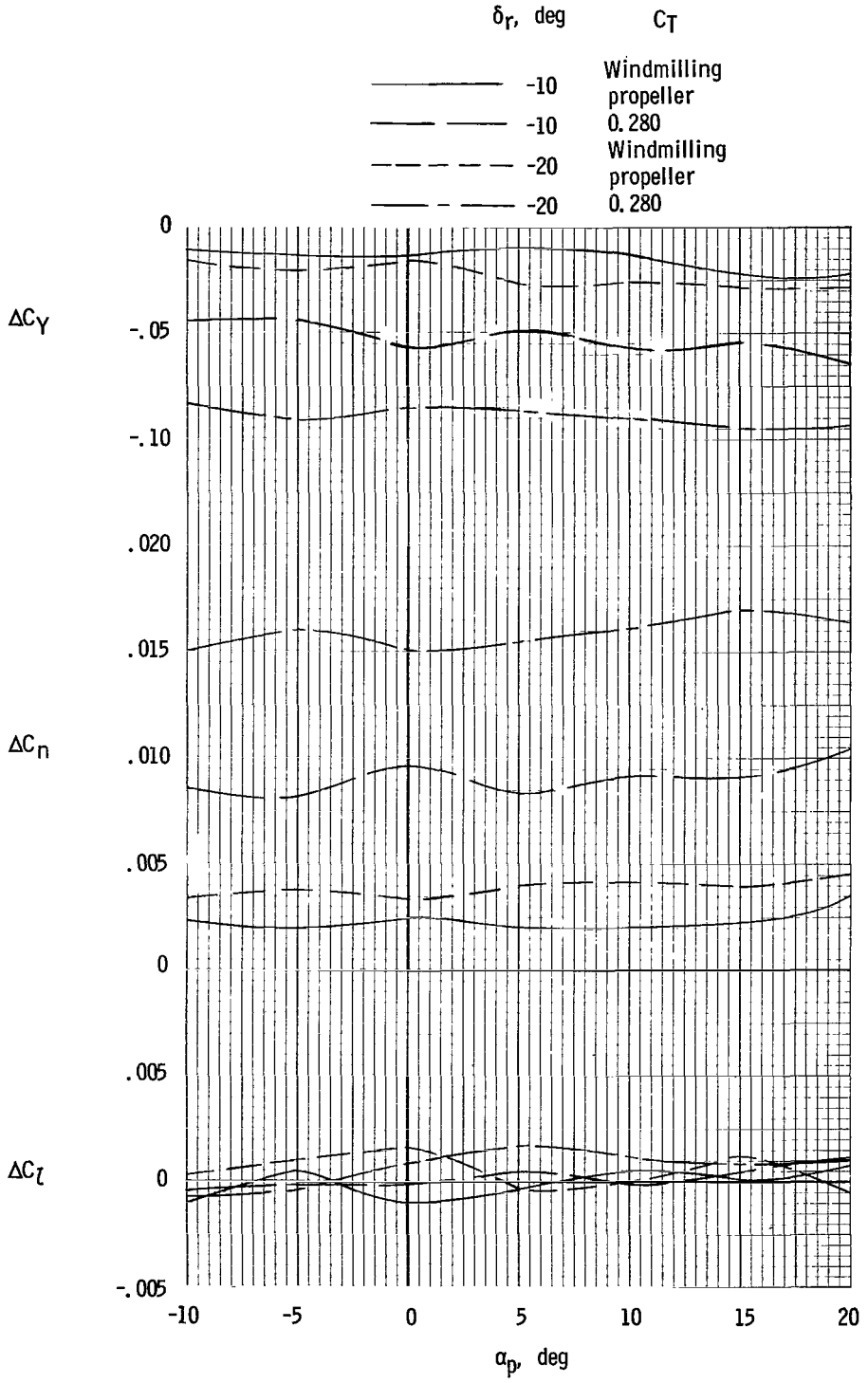

Figure 15.- Incremental lateral forces and moments produced by rudder deflection. $i_w = 25^0$; $\beta = 0^0$.

A motion-picture film supplement L-920 is available on loan. Requests will be filled in the order received. You will be notified of the approximate date scheduled.

The film (16 mm, 7 min, color, silent) shows a free-flight model of an aspect-ratio-6 conical-parawing utility vehicle in level flight using a center-of-gravity-shift control system.

Requests for the film should be addressed to:

Chief, Photographic Division
NASA Langley Research Center
Langley Station
Hampton, Va. 23365

CUT

Date _____

Please send, on loan, copy of film supplement L-920 to TN D-3673

_____
Name of organization

_____
Street number

_____
City and State Zip code

Attention: Mr. _____

Title _____

"The aeronautical and space activities of the United States shall be conducted so as to contribute . . . to the expansion of human knowledge of phenomena in the atmosphere and space. The Administration shall provide for the widest practicable and appropriate dissemination of information concerning its activities and the results thereof."

—NATIONAL AERONAUTICS AND SPACE ACT OF 1958

NASA SCIENTIFIC AND TECHNICAL PUBLICATIONS

TECHNICAL REPORTS: Scientific and technical information considered important, complete, and a lasting contribution to existing knowledge.

TECHNICAL NOTES: Information less broad in scope but nevertheless of importance as a contribution to existing knowledge.

TECHNICAL MEMORANDUMS: Information receiving limited distribution because of preliminary data, security classification, or other reasons.

CONTRACTOR REPORTS: Technical information generated in connection with a NASA contract or grant and released under NASA auspices.

TECHNICAL TRANSLATIONS: Information published in a foreign language considered to merit NASA distribution in English.

TECHNICAL REPRINTS: Information derived from NASA activities and initially published in the form of journal articles.

SPECIAL PUBLICATIONS: Information derived from or of value to NASA activities but not necessarily reporting the results of individual NASA-programmed scientific efforts. Publications include conference proceedings, monographs, data compilations, handbooks, sourcebooks, and special bibliographies.

Details on the availability of these publications may be obtained from:

SCIENTIFIC AND TECHNICAL INFORMATION DIVISION

NATIONAL AERONAUTICS AND SPACE ADMINISTRATION

Washington, D.C. 20546